University of Texas at El Paso
DigitalCommons@UTEP

Open Access Theses & Dissertations

2015-01-01

Accuracy And Precision Evaluation Of Traffic Speed Pavement Deflection Devices

Jorge Velarde
University of Texas at El Paso, javelardemoreno@miners.utep.edu

Follow this and additional works at: https://digitalcommons.utep.edu/open_etd

 Part of the Civil Engineering Commons

Recommended Citation
Velarde, Jorge, "Accuracy And Precision Evaluation Of Traffic Speed Pavement Deflection Devices" (2015). *Open Access Theses & Dissertations*. 1177.
https://digitalcommons.utep.edu/open_etd/1177

This is brought to you for free and open access by DigitalCommons@UTEP. It has been accepted for inclusion in Open Access Theses & Dissertations by an authorized administrator of DigitalCommons@UTEP. For more information, please contact lweber@utep.edu.

ACCURACY AND PRECISION EVALUATION OF TRAFFIC SPEED PAVEMENT DEFLECTION DEVICES

JORGE A. VELARDE MORENO

Department of Civil Engineering

APPROVED:

Soheil Nazarian, Ph.D., Chair

Vivek Tandon, Ph.D.

Calvin Stewart, Ph.D.

Charles Ambler, Ph.D.
Dean of the Graduate School

Dedication

I would like to dedicate this thesis to my parents and sister.

ACCURACY AND PRECISION EVALUATION OF TRAFFIC SPEED PAVEMENT DEFLECTION DEVICES

by

JORGE A. VELARDE MORENO, BSCE

THESIS

Presented to the Faculty of the Graduate School of

The University of Texas at El Paso

in Partial Fulfillment

of the Requirements

for the Degree of

MASTER OF SCIENCE

Department of Civil Engineering

THE UNIVERSITY OF TEXAS AT EL PASO

August 2015

Acknowledgements

I would like to express my gratitude to my thesis and project advisor, Dr. Soheil Nazarian for always having faith in my work and giving me the opportunity to work at the Center for Transportation and Infrastructure Systems. Without his supervision and guidance neither the project nor this thesis would have been possible. His passion and methodology allowed me to discover the passion for pavement engineering I held within. I would also like to express my gratefulness to the Center's staff, especially to Dr. Imad Abdallah, Mr. Jose Garibay and Mr. Sergio Rocha for giving me the opportunity to work along their sides as well as always providing me with the help I needed.

During the development of this project and thesis I had the opportunity to collaborate with other professionals. I would like to extend my gratitude to Dr. Rada, Dr. Sivaneswaran, Dr. Thyagarajan and Dr. Siddharthan.

Also, I would like to thank my thesis committee, Dr. Tandon and Dr. Stewart, for taking the time to review this thesis. I want to thank my fellow CTIS colleagues, particularly Dr. Danniel Rodriguez, Dr. Mehran Mazari; Aaron Arce, Gerardo Garcia, Jorge Beltran and Miguel Perez for the great experiences and advice during those times I needed them the most.

Further, I would like to thank my family especially my father, Jorge R. Velarde and my sister, Itzel Velarde for their unconditional and uninterrupted support. I'd also like to extend my appreciation to my friends for being there and supporting me during all my bachelors and graduate studies.

Abstract

Pavement structural adequacy is considered an important aspect of the pavement management activities and can be incorporated by using surface pavement deflections. Continuous deflection technology, which has been around for several years, can potentially supplant single point deflection measurements provided by the Falling Weight Deflectometer (FWD). Previous studies have evaluated the traffic speed deflection devices (TSDD) accuracy and precision by comparing their results with FWD measurements. Although appropriate correlations and indices to compensate for the differences in load have been made, a direct comparison under the same loading conditions has not been reported in the literature.

The goal of this thesis is to establish a reliable measure of the structural condition of bound pavement layers above the unbound base layer as it deteriorates over time under traffic and environmental loading, based on moving pavement deflection technology, measured at traffic speeds (30 – 60 mph). Two devices, the Greenwood TSD and ARA RWD, were found to be potentially viable devices (Flintsch, 2014). Based on this findings, a work plan was developed and implemented to evaluate whether the two devices met a minimum set of specifications related to the structural evaluation of pavements at the network level, including accuracy and precision of deflection measurements, monitoring applied load, operating speed, and distance between deflection measurements. The modern versions of the TSDDs that are used in this study include the Greenwood Traffic Speed Deflectometer (TSD) and the Applied Research Associates, Inc. Rolling Wheel Deflectometer (RWD).

Table of Contents

List of Tables

List of Figures

List of Illustrations

Chapter 1: Introduction

State Highway Agencies (SHAs) have started considering the structural adequacy of pavements along with pavement distresses and roughness to predict the service life of a pavement. Structural adequacy has been estimated for over 30 years using the results from the Falling Weight Deflectometer (FWD). At present, there is a large array of equipment that can be used to measure the deflection basin that can be used in the calculation of pavement structural indices like the Surface Curvature Index (SCI) and the Modified Structural Index (MSI), Bryce (2013). The most commonly used device in this country since the 1980s has been the FWD. FWDs rely on impact loads to produce a pavement response similar to that produced by actual traffic loadings, which is then measured by deflection sensors located at varying distances from the load. The use of this device will always come with complications like lane closures, time consumption and low frequency of sampling. These shortcomings are especially important in terms of network level pavement management applications, which by their nature require information on a large pavement network measuring in the thousands of miles. To overcome this FWD deficiencies, several engineering companies around the world have developed a way to estimate the surface pavement deflection while traveling at posted traffic speed (up to 60 mph). The modern versions of the Traffic Speed Deflection Devices (TSDDs) that are actively used today include:

- Greenwood Engineering A/S Traffic Speed Deflectometer (TSD).
- Applied Research Associates, Inc. (ARA) Rolling Wheel Deflectometer (RWD).

These devices use non-contact technology to measure the deflection of the pavement generated by a moving vehicle. Previous accuracy studies have evaluated the accuracy of these devices by comparing the results with the FWD. For this study, responses of embedded sensors

into the pavement surface were compared with the deflection parameters obtained from the two devices. The precision evaluation compared the device's results after several repetitive runs over a short period of time. An in-service loop, part of the Minnesota road network, was also tested to simulate real conditions and evaluate the devices' precision. This methodology was developed as part of the FHWA's Project "Pavement Structural Evaluation at the Network Level" (Rada et al. 2015). This thesis will detailed the process of site instrumentation, data collection and data analysis of the embedded sensors and will display the overall results of the two devices. The project field evaluation, took place in the MnROAD facility in Minnesota during September 2014.

1.1 Literature Review

One study developed by Hausman et al. (2011) reported the testing cost reduction of 5% when using a traffic speed deflection devices. He also notice the benefit of knowing the structural capacity of pavements, since surface conditions may not be conclusive. Flintsch et al. (2013) as part of the Second Strategic Highway Research Program (SHRP2) Project R06 evaluated continuous deflection devices to support pavement management decisions. The study identified both the Greenwood TSD and ARA RWD as the two most capable devices of meeting the criteria for accuracy. Field verification for the TSD showed an adequate repeatability with the capability to identify weak pavement spots and that although there was significant variation between deflection measurements and surface indices computed using FWD measurements, the results were broadly comparable. The study recommended several improvements to the devices such as adding supplementary sensors to provide a more complete deflection bowl, measuring pavement layer thickness by adding a ground penetrating radar device and measuring the dynamic load on the wheel assembly (Flintsch et al., 2013). The study also recommended the accuracy of both devices to be evaluated using some type of instrumented pavement sections. Gedafa et al. (2008)

evaluated the accuracy of the Rolling Wheel Deflectometer over 200 road miles in the state of Kansas by comparing structural numbers derived from the FWD and the RWD. Results were highly comparable and recommended a testing frequency of 5 years. Horak (1987) was able to implemented pavement surface deflections in the mechanistic analysis to predict distresses with positive results. Rada et al. (2011) detailed the importance of loading when comparing deflection basins from the TSDDs and the FWD. Recently, Fleming et al. (2015) encountered difficulties when comparing the FWD with a LWD due to the rate of loading and the weight used. An accuracy evaluation under the same loading was recommended. Arora et al. (2006) found that TSDDs and the FWD have similar trends but propose further studies to explain the slightly systematic and unanticipated differences. Bentsen et al. (1989) evaluated the accuracy of seven non-destructive stationary deflection devices by placing a surface geophone adjacent to these devices for the flexible sections and embedding LVDTs on rigid sections. Other studies including the one prepared by Diefenderfer (2010) found a poor correlation between the RWD and the FWD over different pavement structures in the state of Virginia. The precision of the two devices has also been widely studied. Elseifi et al. (2012) along with the Louisiana Department of Transportation studied the RWD precision in various pavement structures resulting in a 15% overall COV and no variation at different speeds. Kelley (2012) established the TSD as a reliable device but emphasis the need to identify unknown influences in the device's performance. Bryce (2012) determined the variance independency from the mean of the measurements, demonstrating the good repeatability over a large range of measurements.

1.2 Device Specifications

The RWD is a continuous deflectometer that can test using a load and loading rate that match the actual dynamic effects on pavements caused by vehicle loading. The RWD utilizes laser

sensors to estimate or measure the maximum deflection between the dual tires of an 18-kip single axle load trailer. The deflection is estimated by comparing the measured undeflected road profile to the deflected road profile at the same location. The RWD is equipped with four laser sensors, with the first three sensors used to measure the undeflected road profile and the fourth sensor to measure the deflection at 7.25 in. behind the center of dual tires at the same location that the undeflected road profile was measured. Two additional sensors were added to measure a second deflection point at a distance of 15 inch forward of the maximum deflection point to estimate the radius of curvature of the deflection basin. The lasers mounted to the RWD device measure at 2-kHz which result in a measurements at approximately every 0.4 in. The average deflection over a 500 ft distance is typically reported. For this study, data was reported at 50 ft average. A picture of the device is presented in Illustration 1.1.

The TSD utilizes Doppler lasers to estimate the so-called deflection velocity of the road profile that is the velocity the pavement deflects due to the moving 11-kip load. The measurements are then divided by the vehicle speed in order to remove measurement dependency on speed, and the output is the pavement deflection slope in millimeters per meter. Since the TSD reports its measured data in SI units, the results were converted to English units for uniformity. The TSD provides deflection velocities at between three and nine points, with the model used measuring at six adjustable distances. Data is typically recorded at a rate of 1000 Hz or 0.8 in. spacing of the raw measurements. Although Katicha et al. (2012) proved that 3 ft average is appropriate for slope measurements, results are typically reported as 32 ft average. Table 1.1 summarizes the three device specifications. A photo of the device is presented in Illustration 1.2.

Table 1.1 Device Comparison Summary

Parameter	ARA RWD	Greenwood TSD
Manufacturer	Applied Research Associates	Greenwood Engineering
Measurement type (Vertical)	Deflection	Deflection Velocity
Measurement location of interest	Behind the centerline of load axle (at 7.25 inches)	Ahead the centerline of the load axle (three locations)
Operation speed	5-60 (mph)	20-55 (mph)
Sampling frequency	0.6 (inch)	0.8 (inch)
Deflection accuracy	2.5 (mils)	4 (mils/s)
Applied load	18 (kips)	11 (kips)
Complete deflection bowl	NO	YES (interpolation necessary

Illustration 1.1: ARA Rolling Wheel Deflectometer

Illustration 1.2: Greenwood Traffic Speed Deflectometer

Chapter 2: Data Collection and Methodology

The main purpose of the field evaluation was to establish the precision and accuracy of the devices considered in this study. This chapter describes the process of collecting, reducing and analyzing the raw data. It also covers different methodologies used to evaluate the precision and accuracy of the two devices.

2.1 Site Selection

MnROAD facility in Minnesota was selected as the primary site since it provided a multitude of test sections in one location. The MnROAD facility consists of a 3.5-mile mainline roadway (Illustration 2.1) comprised of 45 sections with "live traffic" as part of Interstate 94 near Albertville, Minnesota. In addition, a 2.5-mile closed-loop low volume roadway (Illustration 2.2) containing 28 sections is also available. The section lengths are typically about 500 ft. The sections vary in pavement type with the mainline consisting of 13 HMA sections, 15 PCC sections, 14 whitetopping sections and 3 SHRP composite sections and the low volume road consisting of 15 HMA and 13 PCC sections.

In addition to the test sections along the mainline and low volume road of the MnROAD, an 18-mile loop part of Minnesota Department of Transportation (MnDOT) roadway network in Wright County was also tested. The loop was located about 20 miles from the MnROAD facility and separated into nine sections. MnDOT (through Wright County) provided the pavement structure and IRI data in support of the TSDD study. As is the case for many realistic pavement evaluation, a portion of Section 9 was under construction that might have led to unanticipated slow down or lane change in a short segment of that section. In addition to providing realistic test

sections, the loop also contained tight turns and rolling hills that provided data to evaluate the effects of horizontal and vertical curves.

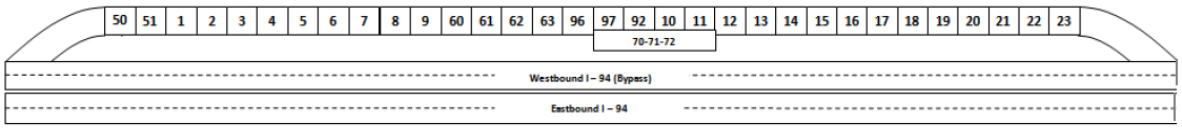

Illustration 2.1: MnROAD Mainline Test Cell Map.

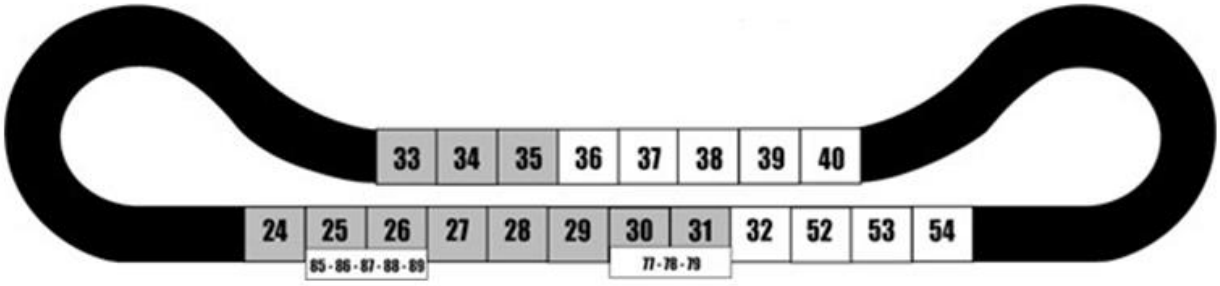

Illustration 2.2: MnROAD Low Volume Road Test Cell Map.

2.2 Site Instrumentation

The MnROAD sections are instrumented with different types of sensors, such as linear variable differential transformers (LVDT), strain gauges, pressure cells, moisture gauges, thermocouples and tipping buckets. For the purpose of this study, these sensors were not used since it focuses only on the surface deflection parameters measured by the TSDDs. Distress surveys, rutting measurements, laser profiler measurements and FWD data are collected regularly on the sections. In addition to those existing sensors, four geophones and one accelerometer were installed as embedded sensors to measure deflection velocity and displacement parameters at four MnROAD cells. Three flexible and one rigid pavement section were selected to evaluate the accuracy of the device over different stiffness pavements. The pavement cross sections for the four cells are included in Illustration 2.3. The three flexible pavement sections covered three levels of

stiffness (Cell 34 soft, Cell 19 intermediate and Cell 3 stiff as judged by FWD testing and pavement structure). Geophones were primarily used since they are the least expensive, can be easily ruggedized in a steel casing, and their one-to-one correspondence to the deflection parameters measured by the TSDDs. In addition, one accelerometer was used at each site to verify the responses of the retrofitted geophones. The geophones had nominal resonant frequencies of 4.5-Hz and a measuring range of 160 mils. The accelerometers were micro-electro-mechanical system (MEMS) DC accelerometer with a nominal sensitivity of 1000 mV/g. The geophones were calibrated using a shaker table and a high precision, reference accelerometer to establish their frequency responses after they were placed in the metallic holders.

Geophones and accelerometers were embedded in the right wheel path of each selected MnROAD cell. Two of the geophones (marked as 1 and 3) were installed along the center of the wheelpath, while the other two (marked as 2 and 4) had 6 inches offset to either side of the wheel path center. The purpose for this offset was to increase the probability of having the test vehicle sensor pass directly on top of one of the sensors while data from the test vehicle and embedded sensors were being collected. The accelerometer was packaged with Geophone 3. The wheel wander for the passes that were used in this study were typically less than 2 inches, so only geophones 1 and 3 were further used in the study.

Sensors were installed at each of MnROAD Cells 3, 19, 34 and 72 – total of 20 sensors. The activities associated with installing the five sensors at each cell included the following:

- Marking the locations of the sensors.
- Coring the pavement down to 2.2 inches or 2.5 inches for sensor containing combined geophone and accelerometer.

- Smoothing the bottom of the holes with an air hammer.
- Grooving the pavement to accommodate the sensor wires.
- Partially grouting the sensors in the core holes.

<table>
<tr><th>Cell 3</th><th>Cell 19</th><th>Cell 34</th><th>Cell 72</th></tr>
<tr><td>3 in. HMA</td><td>5 in. HMA</td><td>4 in. HMA</td><td>9 in. PCC</td></tr>
<tr><td>6 in. Full Depth Reclaimed with Engineered Emulsion Base</td><td>12 in. Unbound Aggregate Base</td><td rowspan="3">12 in. Unbound Aggregate Base</td><td rowspan="3">8 in. Unbound Aggregate Base</td></tr>
<tr><td>4 in. Base</td><td>12 in. Subbase 1</td></tr>
<tr><td>33 in. Subbase 1</td><td>7 in. Subbase 2</td></tr>
<tr><td>Clay</td><td>Clay</td><td>Clay</td><td>Clay</td></tr>
</table>

Illustration 2.3. Accuracy Cells Pavement Structure

The performance of each sensor was then verified using an FWD. For that purpose, one of the FWD sensors was placed directly on top of one of the embedded sensors. The deflections reported by the FWD were then compared with the corresponding deflections reported by the embedded geophones and accelerometers.

The results from this activity, from all fifteen installed sensors at the three flexible MnROAD cells, are presented in Figure 2.1. Results from the rigid section were not included since the slab did not showed a localized deflection basin and results were considered too small to be accurate. The section was removed from further accuracy evaluation. For the rest of the cells, the deflections from the two systems were quite similar. The typical accuracy of the geophones similar to those used in the FWD and installed at MnROAD is reported by the manufacturer as 2% of the

measured deflection (no less than ±0.2 mils). Based on the reported statistics in the figure, on average the FWD and installed sensors' deflections are within about 0.4 mils of one another, which confirms the adequacy of the installed system given the uncertainty associated with measurements with short impulse tests (i.e., FWD).

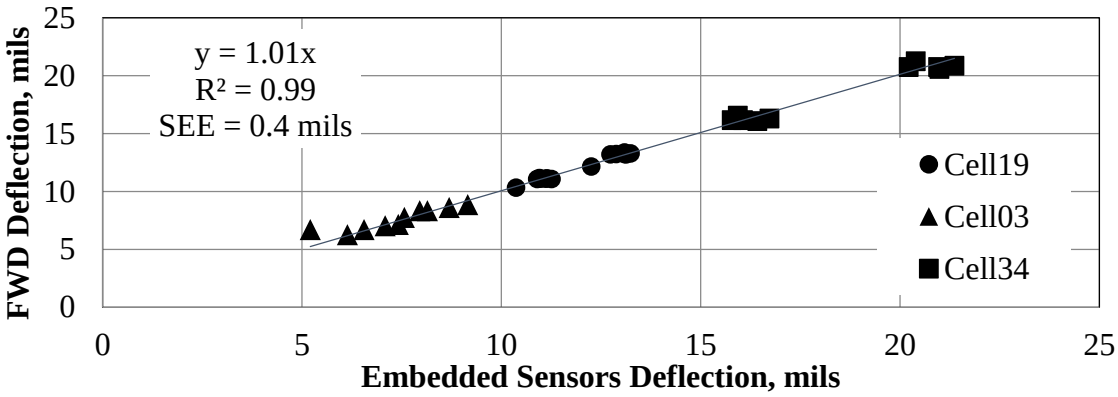

Figure 2.1 Evaluation of Performance of Embedded Sensors using FWD

To properly trigger the embedded sensors, infrared light-emitting diode (LED) positioning sensors were installed in each of the accuracy testing cells. The positioning sensors consisted of a retro-reflective, long-range sensor and a reflector. These sensors had a sensing distance of up to 23 ft and worked with 12 Vdc with an output pulse of the same amplitude.

Markings for the trigger sensor positions were placed on the rest of the cells where accuracy testing was to be done. The data acquisition (DAQ) system program was also modified to capture them in the data files. One positioning sensor was placed directly across from Sensor Unit 3 (geophone 3). The purpose for the trigger placed across Sensor Unit 3 was to use it as a reference to compare the shape of the deflection captured with the embedded sensors and the pulse width created by the tire as it crossed the trigger.

2.3 Data Collection

The DAQ system consisted of a National Instruments USB-6211 and a laptop. The LabVIEW software package, also provided by National Instruments, was used to develop the software needed to acquire, save and analyze the data collected during the testing phase. MnROAD personnel provided an Arbiter Systems GPS clock to ensure the collected data was correctly time-stamped. While the TSDDs did not have this timing system, their computer clocks were sufficient to ensure their data and installed sensors data were correctly matched. To ensure the collected information was correctly assigned, the cell number, TSDD, vehicle speed, surface temperature and repetition number were all part of the naming of the files when data was saved. During data reduction, a problem was encountered while reducing data collected with the accelerometers for 15 out of 64 passes. The problem was tracked down to interference due the absence of a ground connection, and the associated accelerometer data for the 15 passes in questions were dropped from further consideration in the project.

Figure 2.2 shows a typical voltage time history obtained from an embedded geophone, with the peak voltage outputs created by the front and trailing rear axles marked. The time difference between the two peaks was divided by the front axle-to-rear axle distance of each TSDD to obtain accurate instantaneous vehicle speed, assuming that the time lags between the maximum displacement parameters and the time the tire passed over a sensor is constant for the front axle and the trailing rear axle.

The next step of the data analysis was to extract the appropriate range of information from all five newly-embedded displacement sensors, before, during and after the rear axle of the TSDD drove over them over an approximate range of -7 to 10 ft from Sensor Unit 3.

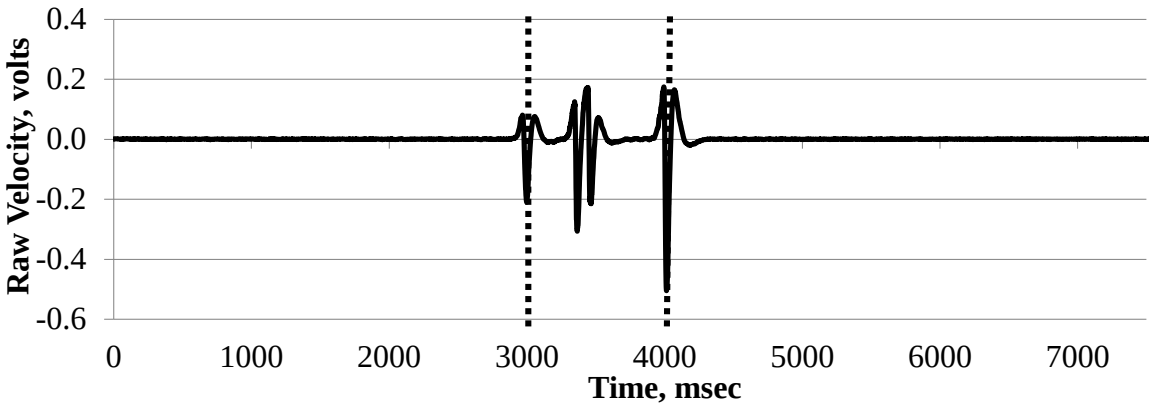

Figure 2.2 Embedded Sensor Full Time History

Since the calibration values of the accelerometers are linear and constant, the accelerometer voltage time history was multiplied by the calibration value to convert it to acceleration. These data were first transformed into the frequency domain using a Fast Fourier Transform (FFT) algorithm, integrated once in the frequency-domain to obtain the velocity spectrum and twice to obtain the deflection spectrum. The velocity or deflection spectrum were then subjected to an inverse FFT to obtain velocity or deflection time histories. The velocity results were compared to the TSD measured values, while the deflection results were compared with the RWD measurements.

The process of analyzing the geophone data involved the use of the nonlinear calibration curve in the frequency domain obtained from the geophone calibration. Since the analysis process had to be done in the frequency domain, the first step was to use a FFT algorithm to convert the selected geophone time history from the time domain to the frequency domain. The shift in the amplitude, especially at low frequencies, demonstrates the importance of implementing a rigorous calibration process to consider the nonlinear behavior of the geophone properly.

The actual velocity spectrum is then subjected to an inverse FFT algorithm to obtain the actual velocity time history that can be compared with those measured by the TSD. At this time, the time axis is also converted to distance as discussed previously.

To obtain the deflection time history, the actual velocity spectrum is integrated in the frequency domain and it is then subjected to an inverse FFT algorithm. Figure 2.3 shows the analysis results from a typical geophone. Discrete results were extracted from the geophones and accelerometer data at spacings that matched the data reported by the TSDDs. For the TSD these distances included 60, 36, 24, 12, 8 and 4 inches from the applied load. For the RWD, two data points at -7.25 and 7.75 inches from the applied load were extracted. Based on figure 2.3 and other similar experiments, the measured deflections with the embedded geophones (and perhaps TSDDs sensors) beyond ± 2 ft are negligible and within the uncertainty band of the measurements.

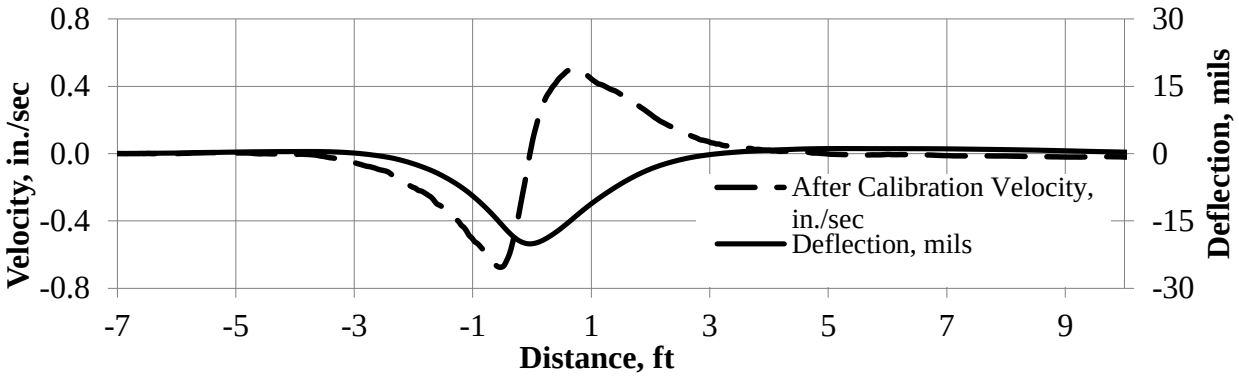

Figure 2.3 Embedded Sensor Full Time History

The peak velocities and deflections estimated from the accelerometer and geophone 3 of each cell (excluding the results from the earlier referenced 15 defective accelerometer records) are compared in figure 2.4 and figure 2.5, respectively. On average, the velocities from the two sensors differ by 3% and the deflections by 7%. Even though accelerometers collect data with less uncertainty than geophones, the fact that the accelerometer raw data have to be integrated twice

introduces more uncertainty in the analyses of deflections. The uncertainties in the reported values as judged by the SEE values are 30 mils/sec and 1.5 mils, respectively. These uncertainties, independent of their sources, were fully attributed to the embedded sensors. Given the uncertainty associated with the data collection and analysis, the results are consistent.

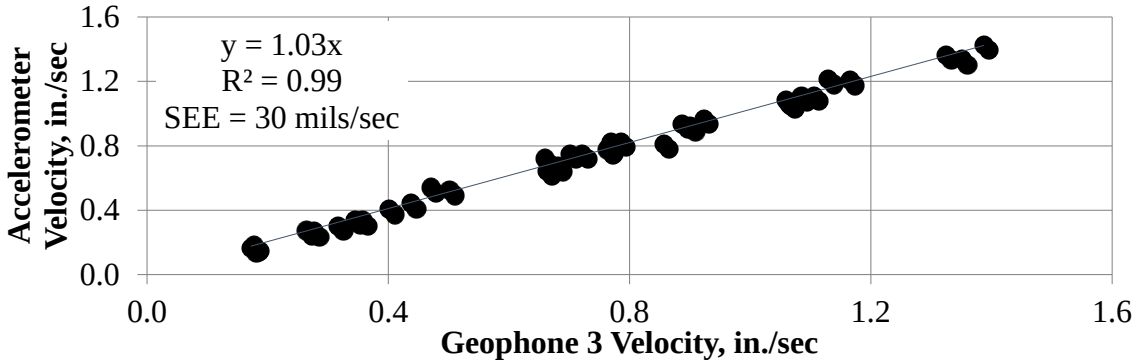

Figure 2.4 Geophone 3 and Accelerometer velocity comparison

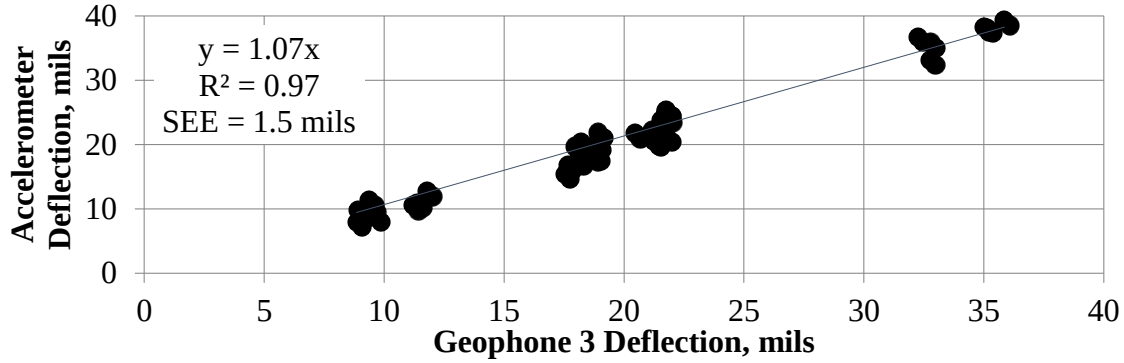

Figure 2.5 Geophone 3 and accelerometer deflection comparison

2.4 Data Analysis

This section will present the methodology followed after data collection and used in the accuracy and precision evaluation of the two devices.

2.4.1 Accuracy

The three HMA cells (3, 19, and 34) were used for accuracy analysis. The deflection measurements from the PCC Cell 72 were not considered because the slab did not show a localized deflection basin and because the magnitudes of the signals reported with the TSDDs and newly-installed deflection sensors were too small to be accurate given their stated uncertainties. The accuracy was established by statistically comparing the results measured with the newly-embedded sensors with those reported by the TSDDs. Since the TSDDs reported their averaged data at 32 ft. for TSD and 50 ft for RWD, one-to-one comparisons of the measured and reported data were not possible for these two devices. As such, the averaged data point closest to the embedded sensors was used for this purpose.

Figures 2.6 through 2.8 are examples that respectively compare the TSD and the RWD discrete measured values with corresponding time histories from the embedded sensors. Since the TSD sensors measures the pavement surface velocity, the velocities measured with Geophone 3 are compared with the TSD velocities in figure 2.6. On the other hand, the accuracy of the RWD was evaluated based on the deflections from Geophone 3 since the RWD reports the surface displacements (see figure 2.7).

The viscoelastic nature of HMA would result in a lag between the time that the tire crosses over the sensor and the time when the maximum response occurs. The deflection parameters shown in figures 2.6 and 2.7 consider such time lags. Figure 2.8 presents the process of obtaining this response lag. First, the most probable time that the center of the tire passed over the sensor was determined by estimating the distance where the trigger signal exhibited a high voltage (i.e., the length that the tire interfered with the LED laser reflection in figure 2.8). The resulting distance was then divided by two to estimate when the tire passed over the sensor (shown with dotted

vertical line in figure 2.8). The lag was then estimated by subtracting the estimated time when the TSDD sensor passed over the embedded sensor from the time when the maximum deflection measured with the geophone (solid vertical line) occurred. After calculating the lag for each pass, all data points were shifted accordingly. The estimated response lags are reported in table 2.1. Given the sampling rate of the newly-installed geophone data and uncertainty in the process used, the uncertainty associated with the estimation of the phase lags are estimated to be 1 to 2 inches. For the RWD passes, the response lags were estimated based on the measured deflections, while for the TSD they correspond to the surface particle velocities. The response lag varied with vehicle speed, temperature and pavement structure.

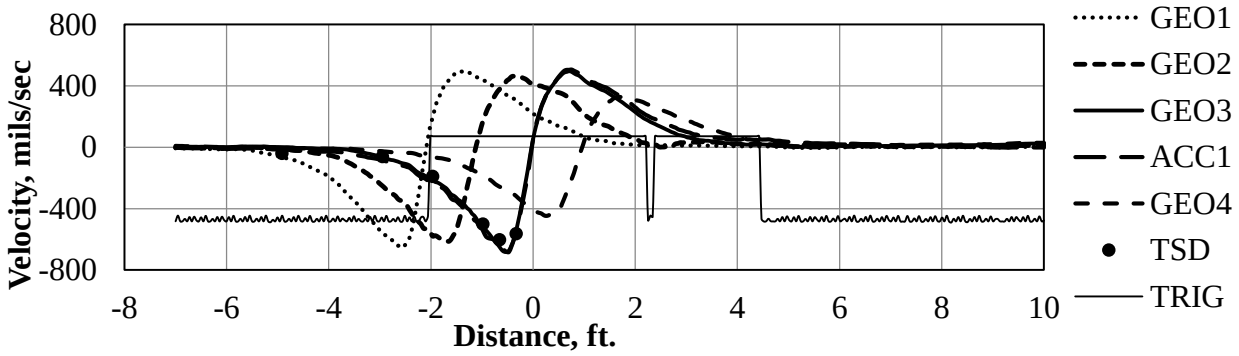

Figure 2.6 Comparison between embedded sensor deflection velocity results and TSD measurements

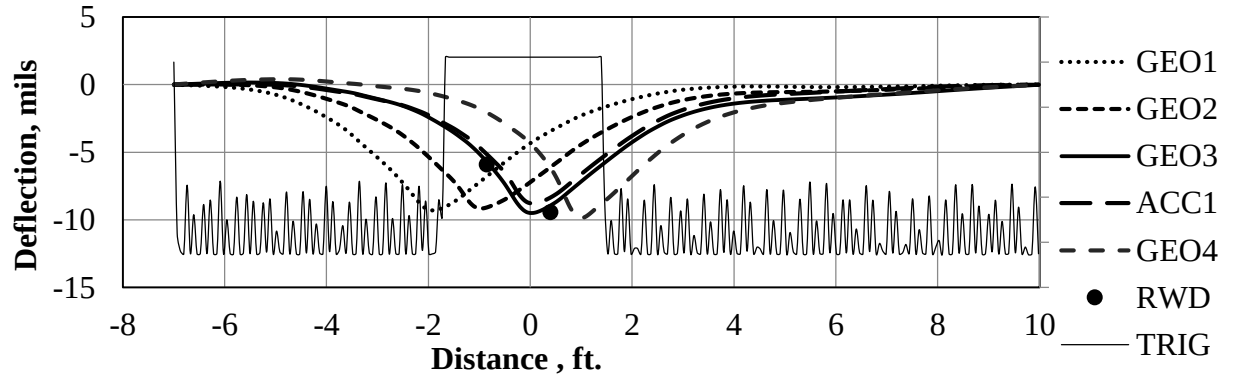

Figure 2.7 Comparison between embedded sensor deflection results and RWD measurements

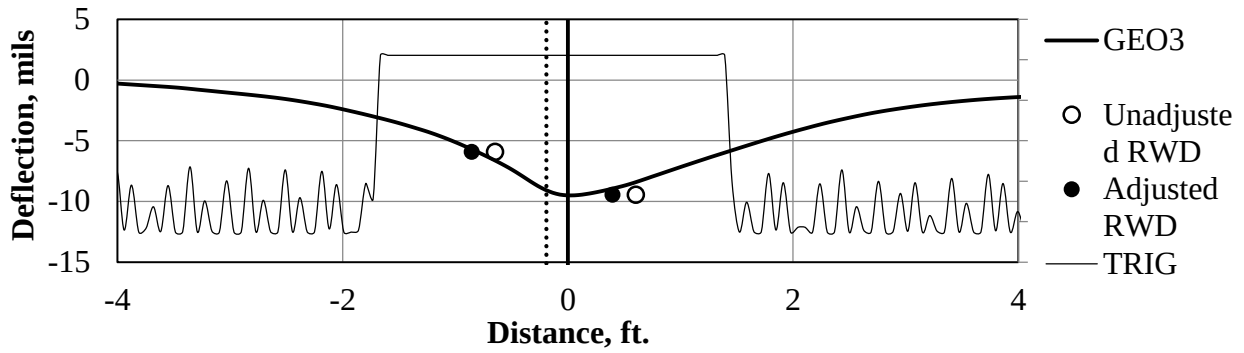

Figure 2.8 Viscoelastic lag calculation

Table 2.1 Pavement Response Lag Results

Cell	Speed (mph)	Response lag (in.)	
		RWD	TSD
34	30	7.3	3.8
	45	6.9	3.4
3	30	4.3	6.6
	45	2.5	5.5
	60	1.6	N/A
19	30	4.5	4.4
	45	3.4	2.8
	60	4.0	2.8

Figures 2.6 and 2.7 show typical comparisons between the parameters reported by the TSDDs and measured by the newly-installed embedded sensors. Given the inherent uncertainty in the acquisition and analyses of the embedded sensors' data, tests were repeated three times at every cell for every TSDD. The results from all three replicates were used to maximize the confidence in the data. The constant and the slope of the best-fit line through the data were used to assess the closeness of the reported and measured results. The intercept measures the bias in the measurements and should ideally be equal to zero. For a fair comparison, the slope, which is an indication of the proportionality of the measurements, should be equal to unity. Average deviation between the measured and reference of a device under a given condition, was also calculated by

determining the absolute difference between the slope of the best-fit line directed through the origin and the line of equality. An average deviation close to zero is desirable. The coefficient of determination (R^2 value) was examined as an approximate surrogate indicator of the scatter in the data since strictly speaking there are uncertainties in both the reference and measured values. Ideally that value should be close to unity. The SEE was judged to be a better indicator of the uncertainty in the results. SEE can be used to estimate how different the deflection parameters from two different pavements should be so that they can be considered different with confidence. The smaller the SEE is, the more subtle changes in pavement structures can be estimated. The individual difference, for sensor i and pass j, e_{ij}, was estimated from:

$$e_{ij} = \text{abs}\left[(d_{ijsensor} - d_{ijTSDD})/d_{ijsensor}\right]$$

where $d_{ijsensor}$ is the deflection parameter (either velocity or deflection) measured with the embedded geophone and d_{ijTSDD} is the deflection parameter reported by the TSDD for its sensor i for pass j.

The average and standard deviation of differences from the three replicates for each sensor were then calculated and reported for each sensor. For TSD, values from the sensor spacings of 36 and 60 in. were not evaluated since their deflection parameters were considered to be too small to be reliably measured by the embedded geophones.

Table 2.2 summarizes the experiments carried out for establishing the accuracy of the TSDDs. The TSD was not able to test Cell 3 at 60 mph because of safety concerns over the breaking distance. Figures and tables similar to those presented were generated for every combination of device, cell and nominal speed shown in table 2.2 but they are not included in the report as they do not provide further insights.

2.4.2 Precision

Precision analysis included almost all cells of the MnROAD facility and the 18-mile Wright County Loop to account for different pavement structures. To better evaluate the precision of the two devices, they were tested at different speeds and at different times of the day. Table 2.3 describes the number of passes, speed and time for each device. Data collection was repeated up to five times at section, for every TSDD and at two different speeds.

Table 2.2 Accuracy Testing Summary

Device	Cell	Nominal Speed (mph)
RWD	3	30
		45
		60
	19	30
		45
		60
	34	30
		45
TSD	3	30
		45
	19	30
		45
		60
	34	30
		45

Table 2.3 Precision Testing Summary

Test Site	TSDD	Passes Per Speed	Speed (mph)	Time
18-mile Loop	TSD	3	Traffic Speed	AM
	RWD	3	Traffic Speed	AM
Mainline	TSD	5	45, 60	AM
		5	45, 60	PM
	RWD	3	45, 60	AM
		3	45, 60	PM
Low Volume Road	TSD	5	30, 45	AM
		5	30, 45	PM
	RWD	5	30, 45	AM
		5	30, 45	PM

Due to safety concerns the low volume road tests were carried out at 30 and 45 mph. These combinations resulted in a total of 78 passes.

The precision analysis for this project started by developing color-coded Google maps. An example of one of the maps is shown in illustration 2.4. The average and COV of the deflection parameters for each sensor from replicate passes were calculated for each reported test point. These values were then color-coded using the convention stated in Table 2.4. This color codification was also applied to the vehicle speed and pavement surface temperature measured by each TSDD since these parameters can influence the precision of the measurements.

Table 2.4 Statistic Map Color Code Legend

Parameter	Green	Yellow	Orange	Red
Measurement	<Avg-StDev	<Avg but >Avg-StDev	<Avg+StDev but >Avg	>Avg + StDev
COV	<5%	<10% but >5%	<20% but >10%	>20%

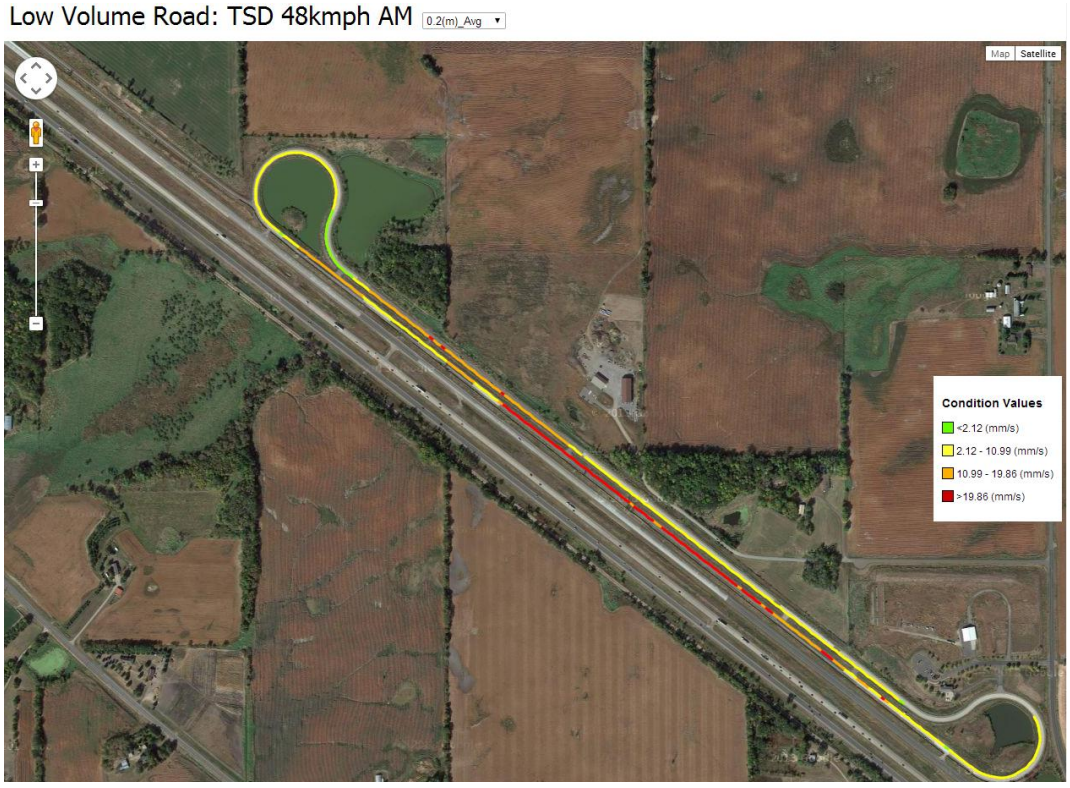

Illustration 2.4 Color Coded Statistics Map

The first step to evaluate the precision was to properly align the starting point of each pass using the GPS coordinates provided by the TSDDs. The second analysis step consisted in comparing the deflection parameters from (3 or 5) replicate passes at similar speeds. For the RWD, the reported surface deflections were used for this purpose. The deflection slope, which is the ratio of the deflection velocity and vehicle speed (instead of deflection velocity that was used for the accuracy study), was used for the TSD. The TSD precision evaluation included the sensors from 4 to 36 in. Unlike the accuracy analysis, which small changes in the deflection parameter may yield high percent differences, the low precision (high variability) of the measurements will impact the analysis of the results negatively. Unlike deflection velocity, deflection slope can potentially reduce the impact of vehicle speed on the results. The appropriate deflection parameters (deflection for RWD; and deflection slope for TSD) from different passes were first plotted and visually inspected to confirm the proper alignment of data (see figure 2.9). In some TSD passes, reported negative numbers were classified as measurement errors and were manually deleted to avoid misleading statistics.

Statistical analyses were then carried out between each two individual pairs of data collected in different passes. As an example, figure 2.10 demonstrates a comparison of the data from the first and second passes of the TSD. Statistical parameters such as the R^2 value, the slope of the best-fit line, and the SEE were estimated for each pair, as shown in table 2.5. To summarize the extracted data in a manageable form, the minimum, maximum and median values of each of these statistical parameters were extracted. These results were then presented as box plots. Box plots demonstrate the ranges, 25 and 75 percentiles and the medians for the slope, R^2, SEE and the range of measured values.

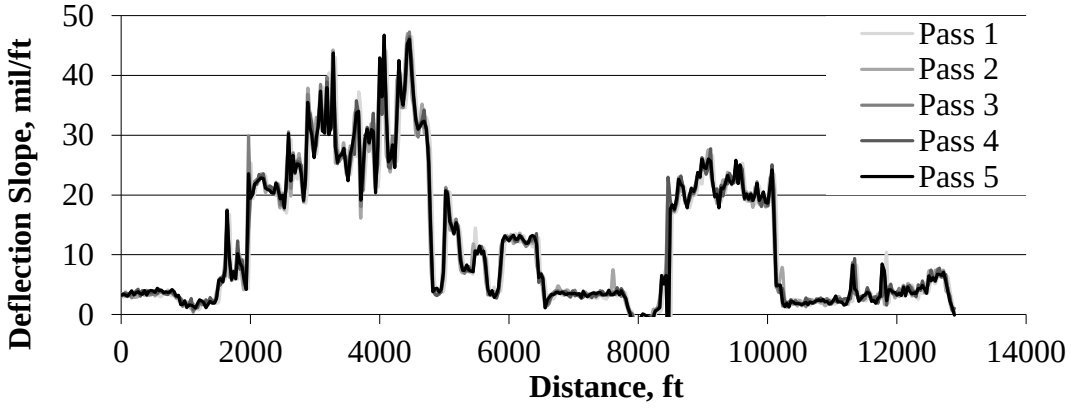

Figure 2.9 Precision Comparison of Passes

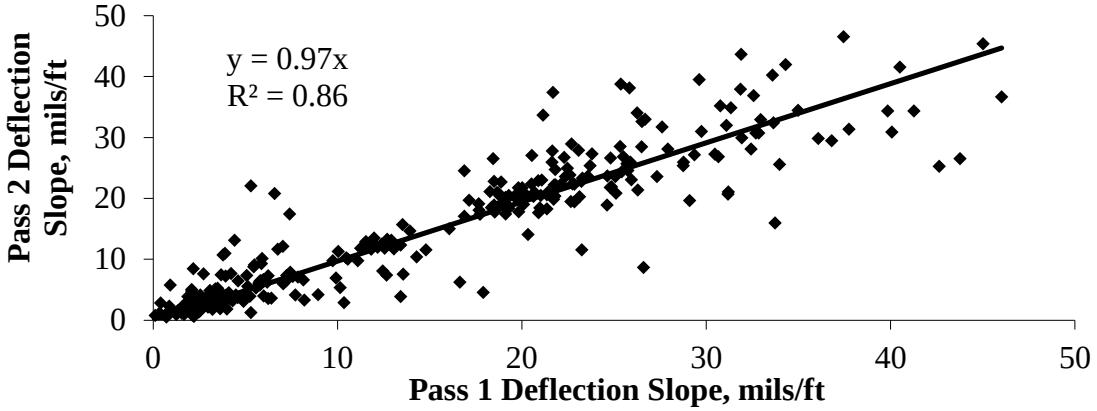

Figure 2.10 Precision Linear Comparison of Passes

Table 2.5 Semi-Triangular Comparison Table

Slope	Pass 1	Pass 2	Pass 3	Pass 4	Pass 5
Pass 1		0.965	0.962	0.972	0.968
Pass 2			0.983	0.987	0.988
Pass 3				0.992	1.003
Pass 4					0.995
Pass 5					
R^2	Pass 1	Pass 2	Pass 3	Pass 4	Pass 5
Pass 1		0.864	0.878	0.911	0.887
Pass 2			0.957	0.965	0.959
Pass 3				0.96	0.997
Pass 4					0.967
Pass 5					
SEE	Pass 1	Pass 2	Pass 3	Pass 4	Pass 5
Pass 1		4.12	3.91	3.34	3.76
Pass 2			2.34	2.08	2.27
Pass 3				2.27	0.65
Pass 4					2.04
Pass 5					

Histograms of the distributions of the reported parameters were also developed to visually evaluate the distributions of the data, as illustrated in figure 2.11.

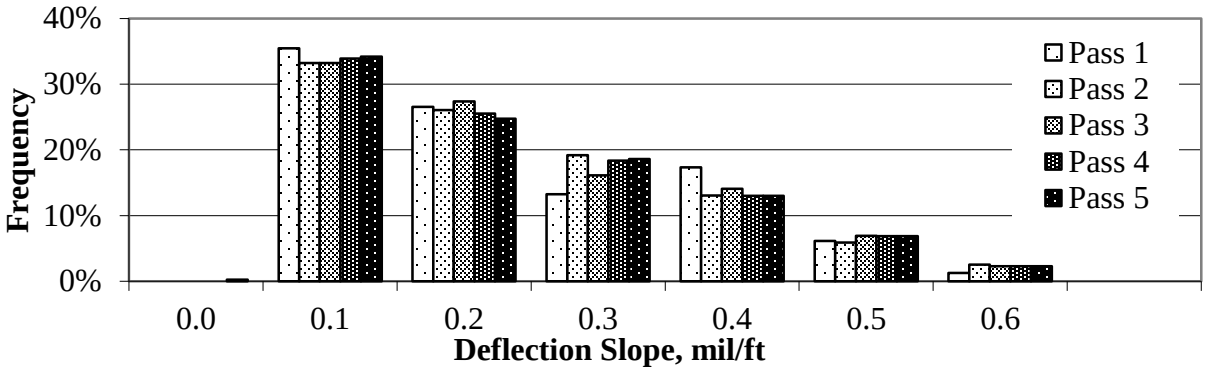

Figure 2.11 Typical Deflection Slope Histogram for a Particular Sensor

Such analyses were performed on the first five sensors of the TSD and the two sensors of the RWD. To further evaluate precision, the different passes were grouped together by time of the day (AM or PM), by speed (30, 45 or 60 mph) and by pavement structure (AC or PCC). These sections used the median COVs of deflection parameters from each sensor within each cell. The COV of the deflection parameter from the three or five test repetitions at each individual data point within each was calculated. The median of these COV values was then extracted and used to avoid a statistical error from single marginal data point.

The variation with pavement structure was defined using the average FWD deflection of the sensor directly under the load (center deflection) normalized to 11 kips. The precision of the device in each cell was also correlated to pavement roughness. The average IRI for each cell (reported by the TSD) during precision testing was used for this purpose. The plots generated for this section were divided into flexible and rigid pavement. The median COVs from different times of day and different speeds were then averaged since this section only focuses on the correlation to pavement structure.

To demonstrate the variation of the precision of the TSD and the RWD with the vehicle speed, the median COVs of the deflection parameter from different passes within a cell of each sensor were calculated at different vehicle speeds. The plots had to be separated between MnROAD Low Volume Road and the Mainline since the precision tests were carried out at different speeds along these two facilities. The Low Volume Road cells were tested at 30 and 45 mph while the Mainline tests were carried out at 45 and 60 mph. The common vehicle speed of 45 mph was used as the common abscissa for reference.

The same procedure as for vehicle speed was followed to estimate the impact of temperature variation on the precision of the TSDDs. Similar plots were developed to compare the median COVs of deflection slopes from morning runs with those from the afternoon runs. Table 2.6 includes the average and COVs of the pavement temperature during precision testing of the TSD and the RWD as measured by the TSD.

Table 2.6 Average Pavement Temperature during TSD and RWD Precision Testing

Test Section	**AM Temperature**		**PM Temperature**	
	Average (ºF)	COV	Average (ºF)	COV
Low Volume Road	68	6.4%	92	5.2%
Mainline	80	9.1%	92	5.4%

Chapter 3: Evaluation of Devices

The purpose of this chapter is to summarize and evaluate the results obtained from analyzing data collected during the field-testing phase of this project based on the work plan in chapter 2. This chapter will provide key findings and conclusions relating to the uncertainty (based on the accuracy results) and variability (based on the precision results) of the TSDDs. The conclusions drawn from the study of the two TSDDs were evaluated further to provide optimum operating conditions and device limitations.

3.1 ACCURACY RESULTS

To quantify these measurements, the discrete values from the embedded sensor and the TSDD were compared against one another to determine the difference in magnitude. Once the data from the TSDDs and the embedded sensors from the cells selected for accuracy testing were analyzed; individual plots for the different TSDDs, at different speeds, and on different pavement structures were generated as described earlier. In each of those spreadsheets, a table presenting a quantitative comparison using the TSDD's sensors and showing the average difference and standard deviation of difference was created as well. The data from these spreadsheets were accumulated to observe the overall TSDD behavior through the various speeds and pavement structures. The texture of the pavement surface are known to impact the accuracy of the measurements. This parameter was not studied in this project.

The overall results from the two devices are individually discussed next. However, it would be prudent to discuss the limitations associated with this assessment. As indicated before, the uncertainty associated with the measurement with the geophones is specified by the manufacturer as ±2% of the measured deflection (no less than ±0.2 mils). Given the uncertainties associated with

the data analysis and alignment of the TSDDs over the sensors and imperfections in installation are on the order of ±7% with standard error of estimates of 150 mils/sec for velocity and 1.5 mils for deflection. It would have been desirable to carry such comparisons with more refined data from the TSDD's. Neither of the two TSDDs provided raw measurements of their data. The uncertainties associated with the measurements reported by the TSDDs are by far greater than those reported by the embedded sensors given the spatial standard deviations reported by the RWD and the typical raw data reported by Flintsch et al. (2012) for TSD. As such, the results provided herein should be considered reasonable.

3.1.1 RWD Accuracy Results

The process followed to evaluate the RWD from each pass was discussed in Section 2.4.1. Table 3.1 contains the overall results obtained at different instrumented cells and at different speeds for the RWD. The column referring to constant can be used to observe whether there is a device related systematic (e.g., due to sensor calibration) difference in measurements. Since the constant values change with the cell and vehicle speed, the uncertainties in the measurements cannot be considered systematic. The slopes of the best-fit line vary from 0.84 to 2.41 indicating moderate to significant variability from unity desired from a perfect device.

The R^2 value should ideally be close to unity. That is the case for Cells 19 and 34 (the two less stiff sites), but it is not for Cell 3 (the stiffest flexible site). The SEE is 1.5 mils or less for the two less stiff cells and 2.0 mils and greater for the stiffest Cell 3. Average deviation for the stiffest site (Cell 3) varies from 10 to 38%, while for Cell 19 and 34 the maximum average deviations are 7% and 17%, respectively. Again, about 7% of the average deviation can be due to the uncertainties in the data collection and analysis of the embedded geophones' records. The SEE in

conjunction with the range of deflections is particularly important to assess the minimum level of changes in deflection or damage that the device can delineate.

Table 3.1 RWD Overall Accuracy Statistics

Cell	Speed (mph)	Overall Statistics				
		Constant, mils	Slope	R^2 Value	SEE, mils	Average Deviation
3	30	-2.9	1.68	0.70	2.0	29%
3	45	-3.4	1.83	0.68	2.2	38%
3	60	-12.0	2.41	0.71	2.3	10%
19	30	1.0	0.91	0.96	0.9	2%
19	45	2.7	0.89	0.89	1.5	7%
19	60	-0.1	1.07	0.88	1.4	7%
34	30	6.2	0.84	0.99	0.6	17%
34	45	4.6	0.89	0.98	0.9	15%

As discussed in Section 2.4.1, another way of evaluating the TSDDs is by calculating the difference associated with each sensor. Table 3.2 contains that information from all experiments. The average differences from the replicate tests at each cell and speed varied between 7% and 145%. The median differences for the two sensors were 14% and 15%. The median was reported as opposed to the average to ensure that the occasional outlying data do not disproportionately impact the interpreted accuracies.

Figure 3.1 shows the overall plots obtained from the evaluation of the RWD. Overall the RWD deflections are 11% greater than the embedded sensors. Figure 3.1 also includes 95% confidence and prediction intervals. The confidence interval means that there is 95% probability that the population will lie within the confidence interval of the regression line calculated from the sample data. However, prediction interval is a range that is likely to contain the response value of a new observation given the linear regression model chosen.

Table 3.2 RWD Accuracy Statistics for Individual Sensors

Cell	Speed (mph)	Difference of Sensor at -7.25 in.		Difference of Sensor at 7.5 in.	
		Average	Standard Deviation	Average	Standard Deviation
3	30	69%	23%	68%	36%
3	45	83%	33%	82%	20%
3	60	145%	28%	137%	31%
19	30	9%	5%	10%	7%
19	45	11%	5%	13%	16%
19	60	9%	8%	7%	9%
34	30	16%	2%	16%	6%
34	45	11%	3%	11%	10%
Median		14%	--	15%	--

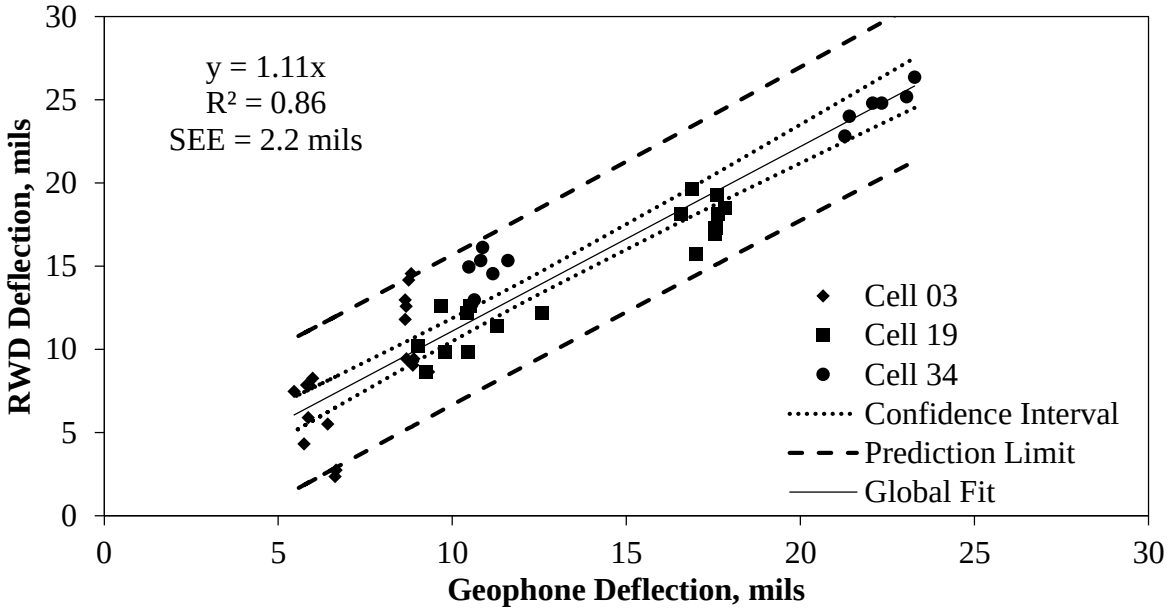

Figure 3.1 Overall Comparison of Deflections Measured with RWD and Embedded Sensors

The impact of the vehicle speed on the performance of the RWD is demonstrated in figure 3.2. The y-axis corresponds to the median difference measured at all cells at a certain speed. Both sensors' median differences were higher when the RWD was operated at 60 mph than the other two lower speeds.

The cell stiffness seems to impact the performance of the RWD as presented in figure 3.3. Sufficient data are not available to define reason(s) for this impact. The stiffest section (Cell 3)

demonstrates a median difference ranging from 70% to 140%. Cell 19 had the smallest median difference of less than 10% for the three speeds. The median values are considered to minimize the uncertainties in the reported values related to occasional outliers observed during analysis.

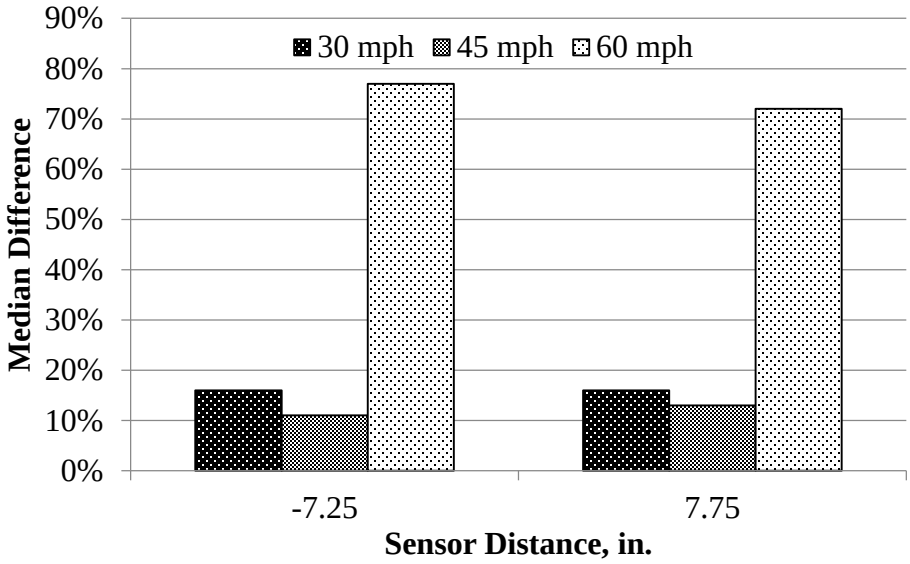

Figure 3.2 Median Sensor Difference for RWD with Varying Speed

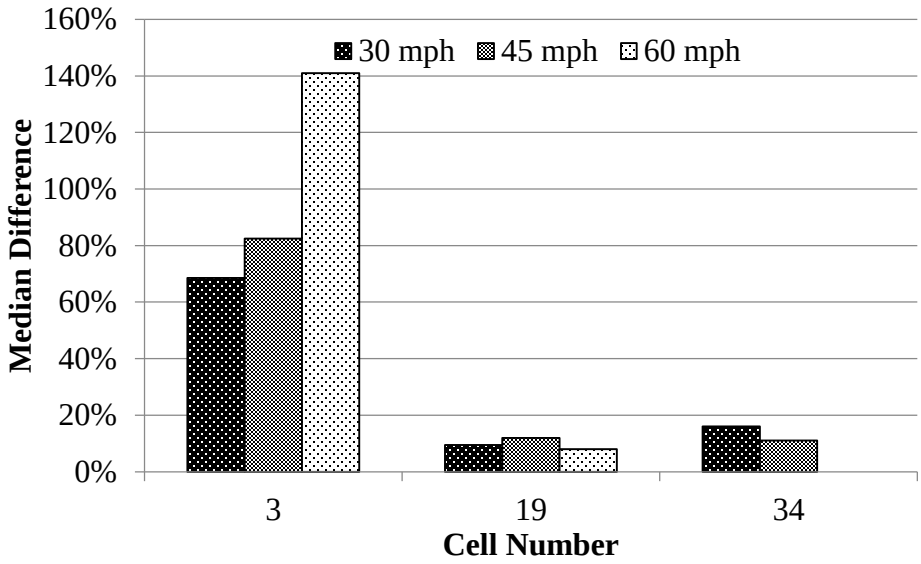

Figure 3.3 Distributions of Deflections Difference Measured with RWD for each Cell

3.1.2 TSD Accuracy Results

As indicated above, the parameter measured with a TSD is termed deflection velocity (particle velocity of the pavement surface). As such, a similar procedure as discussed for the RWD was followed to evaluate the TSD in terms of the deflection velocity. Table 3.3 depicts the overall results based on the deflection velocities. The evaluation is limited to those sensors that are 24 inches or less from the load since the deflections measured with the geophones and the TSD farther than that distance are considered to be too small to be sufficiently reliable.

Table 3.3 TSD Overall Accuracy Statistics

Cell	Speed (mph)	Overall Statistics				
		Constant (mils/sec)	Slope	R^2 Value	SEE (mils/sec)	Average Deviation
3	30	78.80	0.96	0.47	48.66	42%
3	45	61.37	1.11	0.66	64.29	34%
19	30	163.29	0.86	0.80	83.59	21%
19	45	109.10	0.94	0.97	44.88	9%
19	60	97.26	0.97	0.93	89.16	7%
34	30	225.83	0.81	0.92	90.32	6%
34	45	190.90	1.00	0.99	35.43	17%

The constants from the best-fit lines vary between 60 mils/sec and 225 mils/sec. Given the narrow range, the difference may be partially systematic and hence it may be possible to improve them with a more rigorous calibration of the device. For that reason, those constant values, were considered as systematic in the calculations of the differences in table 3.4. The slopes of the best-fit lines vary between 0.81 and 1.11, which is fairly close to the ideal value of unity in most cases. The R^2 values are reasonably close to unity except for the stiffest section (Cell 3). The SEE values vary between 35 mils/sec and 90 mils/sec, and they seem to increase as the pavement becomes less stiff. The stiffest section (Cell 3) had the highest average deviation (over 34%). The average deviation for the less stiff cells is small with the highest value being 17%. Up to 7% of these

average deviations can be explained by the uncertainty of the data collection and analysis with the embedded sensors.

The average and standard deviation of differences of each individual sensor are presented in table 3.4. In terms of velocities, sensors located at 4, 8 and 12 inches away from the applied load seem to match the embedded geophones' responses better with median differences of 13%, 10% and 9%, respectively. Once again, the median values are considered to minimize the uncertainties in the reported values related to occasional outliers observed during analysis. The differences for sensors located farther than 24 inches from the applied load were in excess of 25%.

Table 3.4 TSD Accuracy Statistics for Individual Sensors

Cell	Speed (mph)	Difference of Sensor at							
		4 in.		8 in.		12 in.		24 in.	
		μ	σ	μ	σ	μ	σ	μ	σ
3	30	18%	5%	11%	4%	35%	12%	51%	23%
3	45	1%	1%	15%	17%	49%	16%	28%	7%
19	30	26%	11%	10%	6%	9%	4%	52%	26%
19	45	12%	1%	2%	2%	2%	1%	13%	10%
19	60	13%	5%	3%	3%	6%	6%	11%	11%
34	30	25%	10%	16%	10%	10%	11%	45%	9%
34	45	2%	2%	2%	1%	3%	4%	5%	7%
Median		13%	--	10%	--	9%	--	28%	--

μ = mean value, σ = standard deviation

The TSD deflection velocities are compared with the corresponding deflection parameters from the embedded geophones in figure 3.4. The slope of the global fit depicts a difference of about 12%. This and an R^2 value of 0.94 demonstrate the overall level of performance of the TSD. Most of the data points fall close to the global fit, generating a tight confidence interval and prediction limit with an SEE of about 80 mils/sec.

Sensors were also evaluated with varying vehicle speeds. Results are given in figure 3.5. The median difference is the greatest for vehicle speed of 30 mph and usually the least at 45 mph.

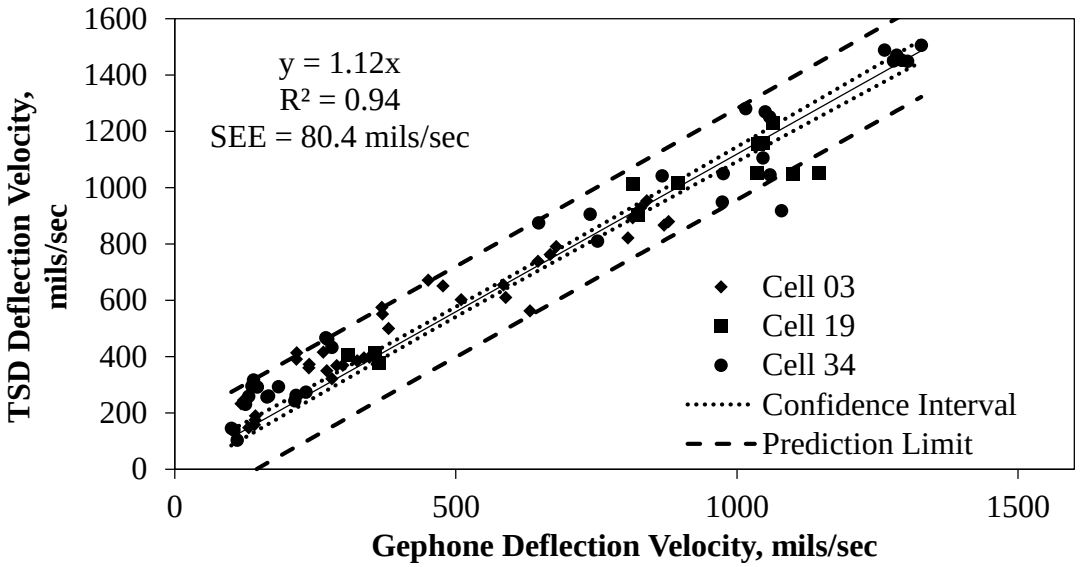

Figure 3.4 Overall Comparison of Deflections Measured with TSD and Embedded Sensors

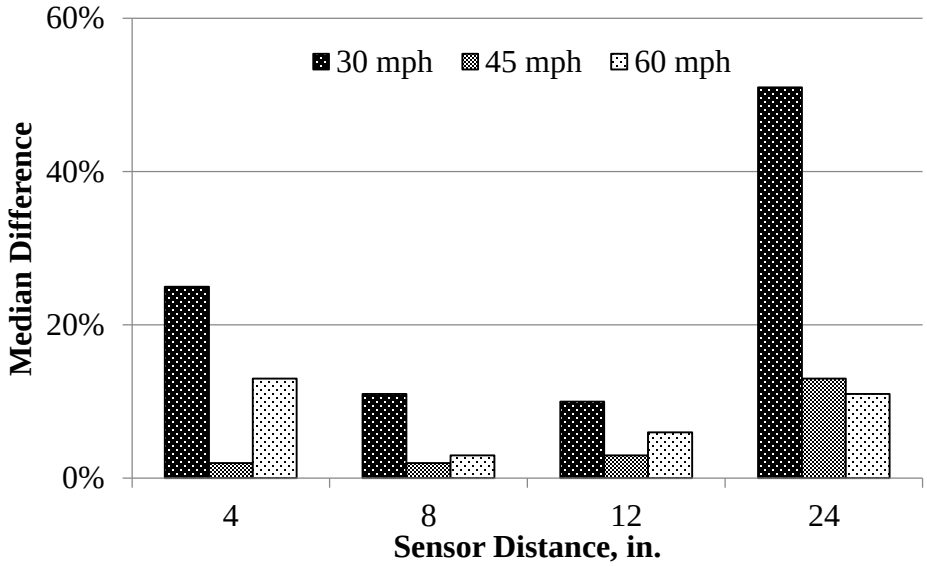

Figure 3.5 Median Sensor Difference for TSD with Varying Speed

The variations in differences with pavement structure are summarized in figure 3.6. Median differences were obtained from all of the sensors' differences except for the one at 36 and 60

inches. The stiffest cell (Cell 3) had a median difference ranging from 22% to 27% at two different speeds. Cells 34 exhibited the lowest median difference (around 3%) at 45 mph.

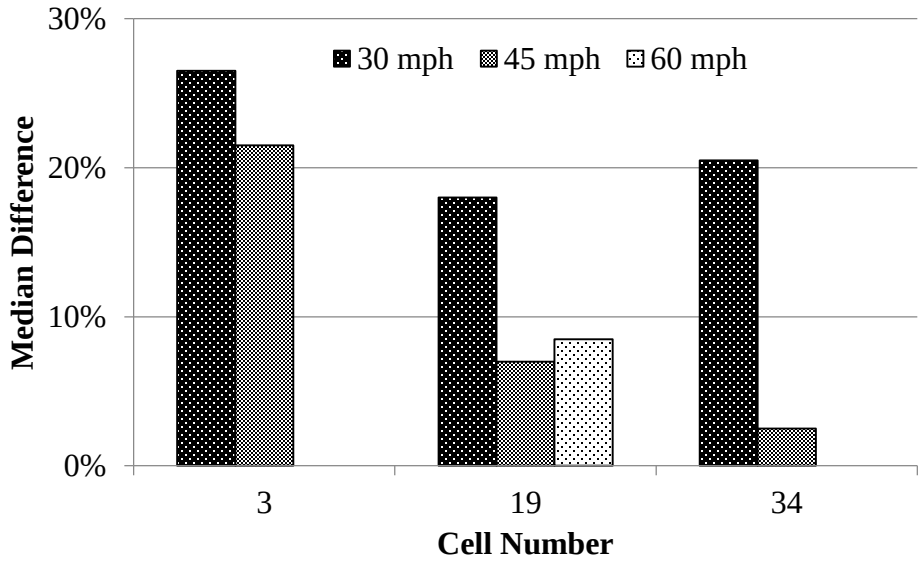

Figure 3.6 Distributions of Deflections Difference Measured with TSD for each Cell

3.2 PRECISION RESULTS

The evaluation of the precision was carried out by analyzing the results obtained as discussed in Section 2.4.2 for almost all MnROAD cells and the 18-mile loop. To evaluate the influence of speed, temperature, and pavement structure and roughness in precision, each individual cell was also analyzed so that the variation in precision could be directly related to each of those factors. Several other factors such as the road geometry (slope and curves) were also studied less quantitatively using the TSD's 18-mile loop data. Some other parameters such as the surface texture that are known to impact the precision could not be studies due to the lack of texture data. The results are discussed next.

The RWD deflections were directly used for the precision analysis. However, the deflection slopes (i.e., deflection velocity divided by the vehicle speed) were used instead of the

deflection velocity for the evaluation of TSD to reduce the speed-related variability in the results. The data from the TSD sensor placed at 60 inches from the load were not considered in the precision analysis due to its high variability and small reported values.

Box plots were developed to delineate the median, upper and lower quartiles and minimum and maximum values. The y-axis consisted of the slope, R^2 value, SEE (as discussed in Section 2.4.2) and the range of measured values for all sections at all three speeds and during morning and afternoon. The precision of each sensor was evaluated individually.

3.2.1 RWD Precision Results

Overall results from the RWD along the MnROAD Low Volume Road and the Mainline are presented in figure 3.7 through figure 3.14. The reported RWD data related to the PCC sections were limited to seven sections. As such, the results reported here are more relevant to the flexible and composite sections.

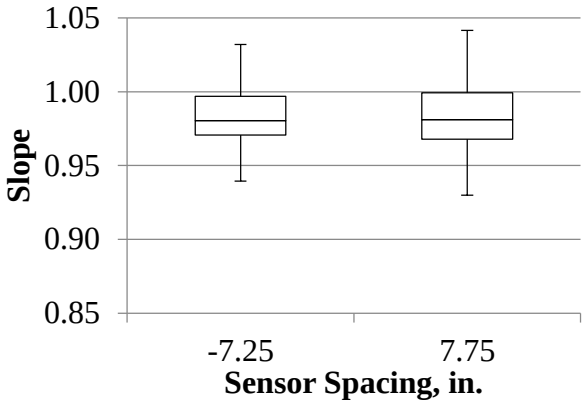

Figure 3.7 RWD Overall Precision Slope in the Low Volume Road

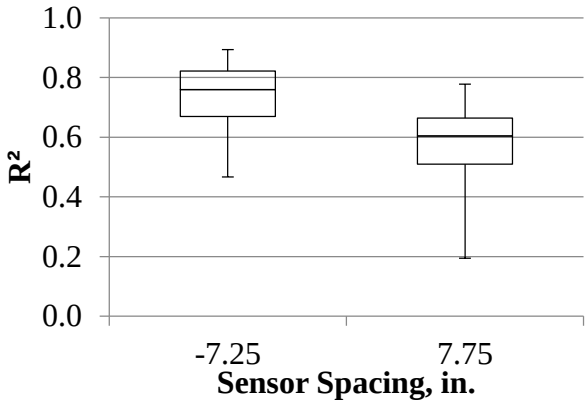

Figure 3.8 RWD Overall Precision R^2 in the Low volume Road

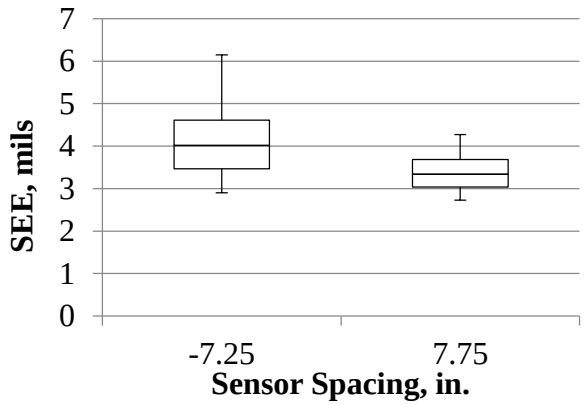

Figure 3.9 RWD Overall Precision SEE in the Low Volume Road

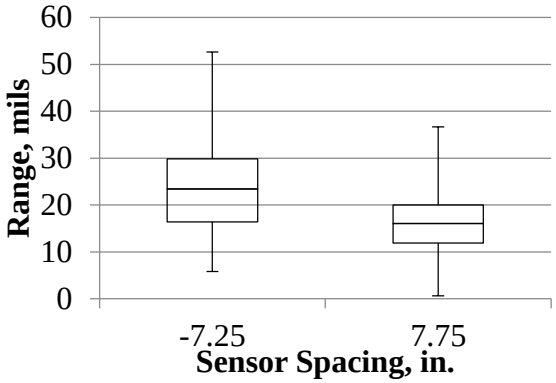

Figure 3.10 RWD Overall Precision Range in the Low Volume Road

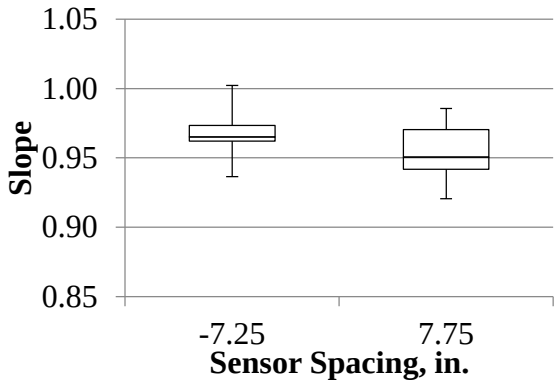

Figure 3.11 RWD Overall Precision Slope in the Mainline

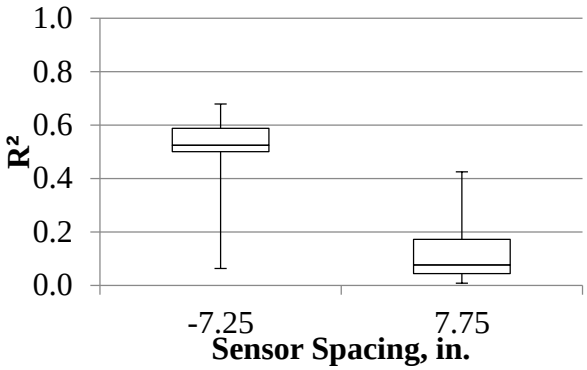

Figure 3.12 RWD Overall Precision R² in the Mainline

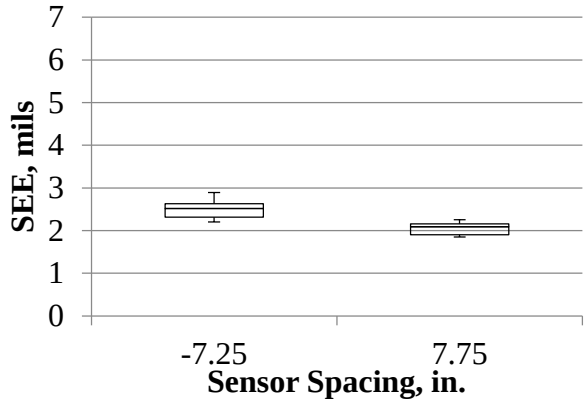

Figure 3.13 RWD Overall Precision SEE in the Mainline

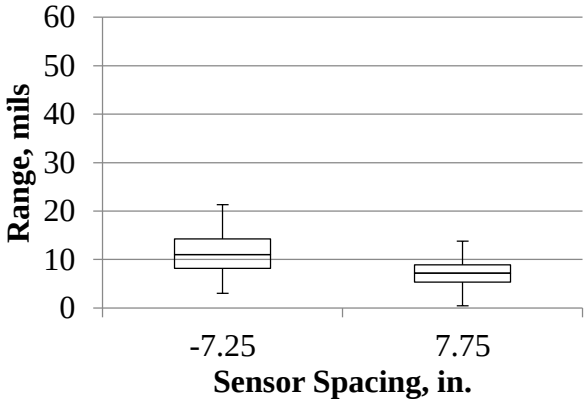

Figure 3.14 RWD Overall Precision Range in the Mainline

With slopes between the deflections from different passes averaging above 95%, both sensors exhibited satisfactory overall reproducibility. However, the median R^2 values of 0.8 and less, point to high scatter among deflections collected at each test point amongst different runs. The sensor located at 7.25 inches behind the axle exhibited greater R^2 values, especially along the Low Volume Road.

The median SEE from relating the deflections from different passes and sensors were 4 mils or less. The uncertainty of the measurements can be evaluated by comparing the SEE with the range of deflections measured along the test sections. The median deflections were 24 mils or less for the sensor behind the axle and 16 mils or less for the sensor located at 7.75 inches in front of the axle. As such, the median SEE is about 15% to 25% of the median deflections measured by sensors.

Figure 3.15 through figure 3.18 depicts the Wright County 18-mile loop overall results, including only the minimum, median and maximum. The upper and lower quartiles are not shown because the experiments consisted of only three passes. Overall the RWD exhibited a reasonable performance when tested under realistic environment. The slopes of the relationships among different passes are typically 0.95 or better, which are close to the ideal value of unity. The R^2 values are also above 0.86 for both sensors. The median SEE values are about 10% of the median deflections for the sensor 7.25 inches behind and about 15% for the sensor located 7.75 inches in front of the load. It should be mentioned that the data provided for the 18-mile loop was averaged over 0.1 mile, whereas the data used in the precision and accuracy along the MnROAD was provided at 50 ft intervals. This may explain the apparent higher precision of the RWD along the 18-mile loop as compared to the MnROAD sections.

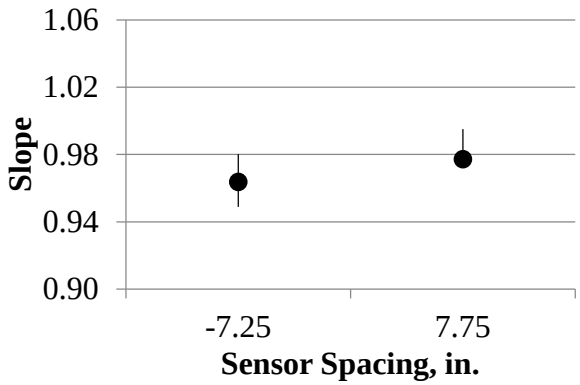

Figure 3.15 RWD Overall Precision Slope in the 18-Mile Loop

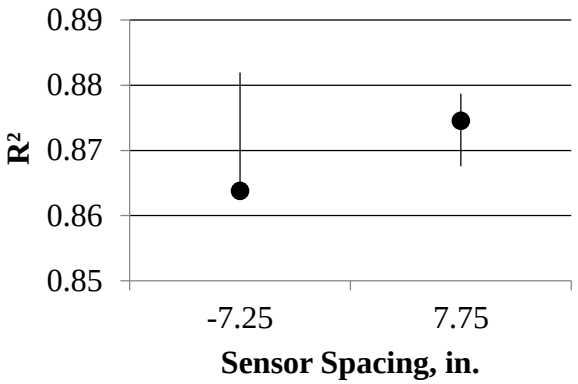

Figure 3.16 RWD Overall Precision R² in the 18-Mile Loop

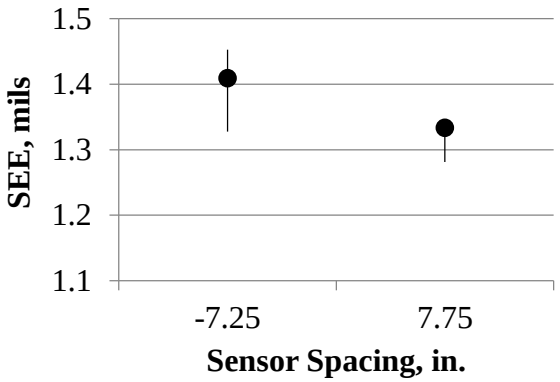

Figure 3.17 RWD Overall Precision SEE in the 18-Mile Loop

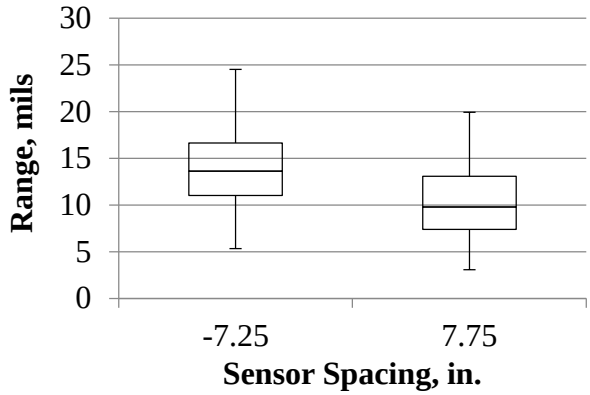

Figure 3.18 RWD Overall Precision Range in the 18-Mile Loop

Figures 3.19 and 3.20 present the trends between the median coefficients of variation of deflection for each cell with the average FWD central deflection (as an indicator of the structural stiffness of each cell). As the FWD deflection increases (i.e., the cell becomes structurally weaker) the COV of the RWD measurements tend to decrease (i.e., the precision of the RWD increases). Based on limited accuracy data, the accuracy of the RWD measurements also decreased with the increase in stiffness.

Figures 3.21 and 3.22 depict the comparison between the RWD median coefficient of variation of deflection and IRI. It is difficult to draw a conclusion on the influence of the IRI on the precision of the RWD given the scatter in the results.

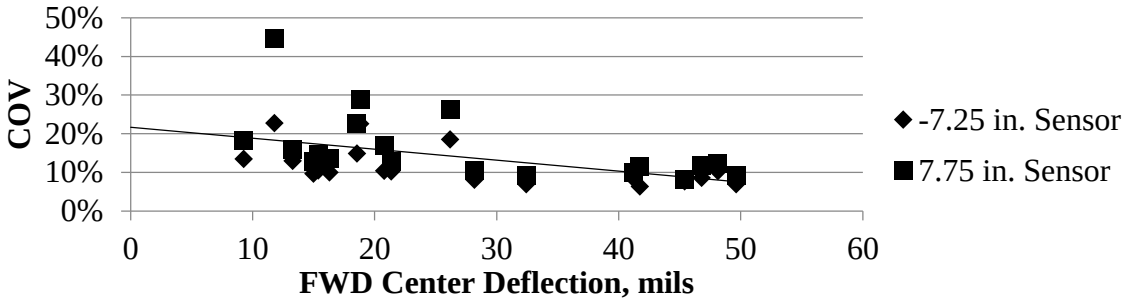

Figure 3.19 Precision Variation of RWD with Pavement Stiffness over Flexible Pavement

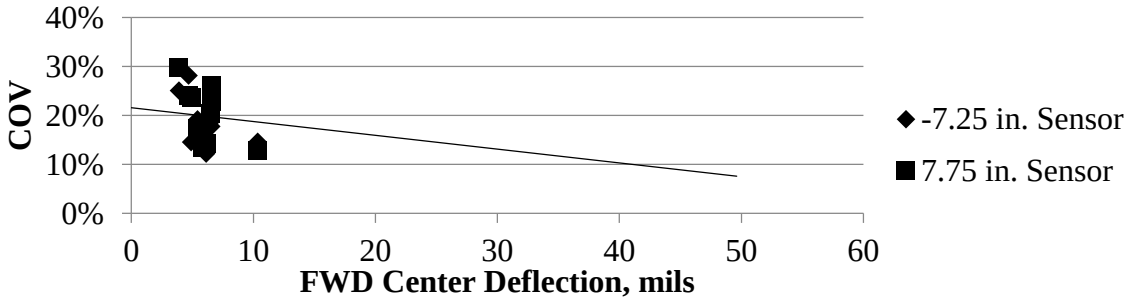

Figure 3.20 Precision Variation of RWD with Pavement Stiffness over Rigid Pavement

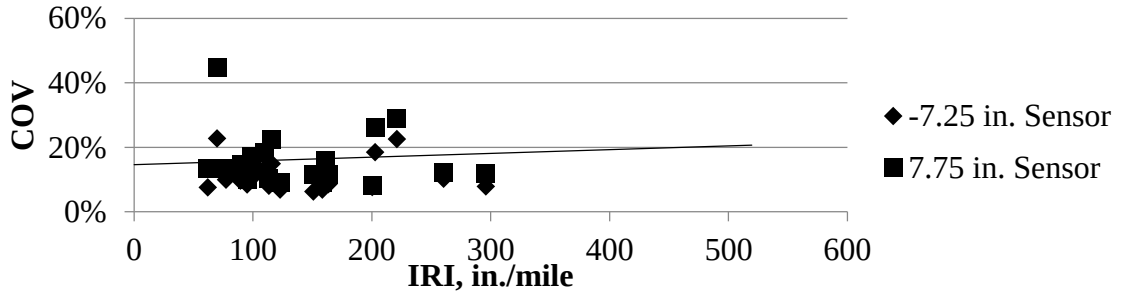

Figure 3.21 Precision Variation of RWD with IRI over Flexible Pavement

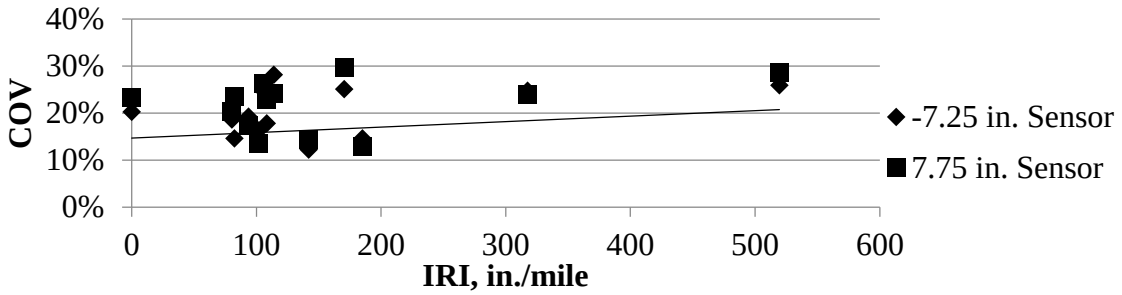

Figure 3.22 Precision Variation of RWD with IRI over Rigid Pavement

Based on the slopes of the best-fit lines shown in figure 3.23 and figure 3.24, the RWD becomes mildly (5% to 10%) less precise as the operational speed increases. The relationship shown in figure 3.23 for the Low Volume Road cells are stronger (i.e. exhibits higher R^2) than the relationship from Mainline cells shown in figure 3.24. This trend can be attributed to the fact that the Mainline cells are generally stiffer than the Low Volume Road cells. The RWD seems to exhibit more precise measurements at lower speeds. Although measurements are not highly affected by vehicle speed, the optimum operational speed should be the slowest one that is a compromise between operational costs and safety. Similar results were observed in figure 3.2 where the performance of the RWD is also negatively affected at vehicle speeds of 60 mph.

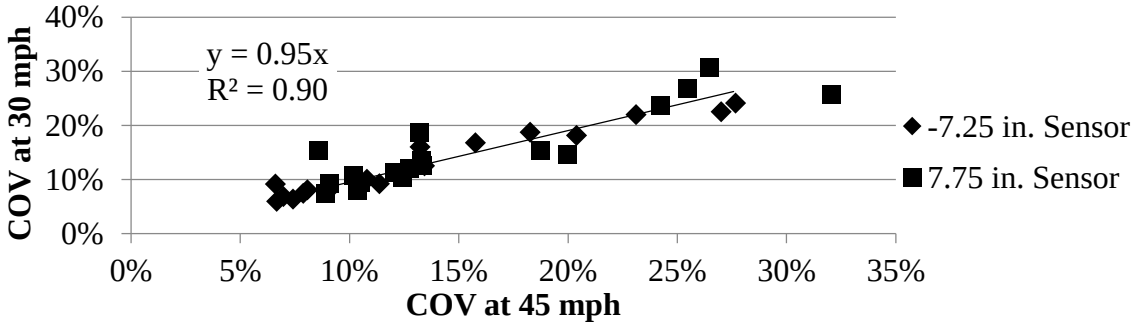

Figure 3.23 Precision Variation of RWD at Different Speeds in the Low Volume Road

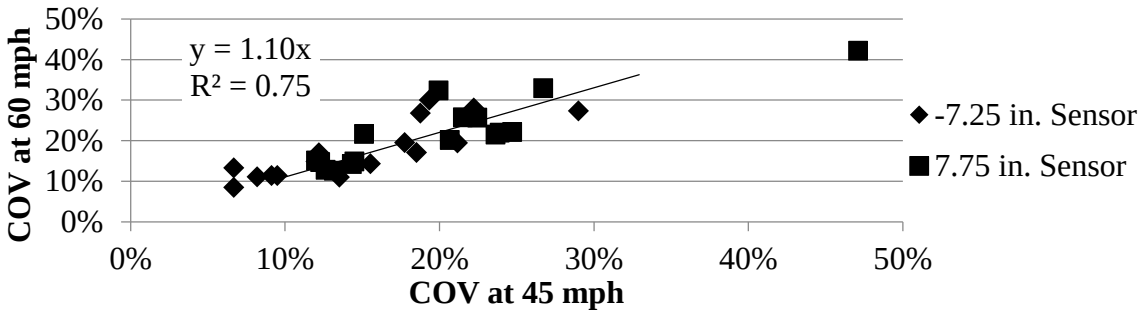

Figure 3.24 Precision Variation of RWD at Different Speeds in the Mainline

RWD temperature induced precision variation results are presented in figure 3.25. A weak correlation between the afternoon and morning COVs of the deflections can be observed considering that the R^2 value is 0.61. Afternoon runs turn out to be around 7% more precise than morning runs. One reason for this pattern can be that high temperature creates a softer surface layer that increases the measured deflections. For the same sensors, one expects higher precision as the measured parameter increases. RWD consistently showed lower precision when the measured deflections were small for stiffer pavement or when the device was operated at higher vehicle speed.

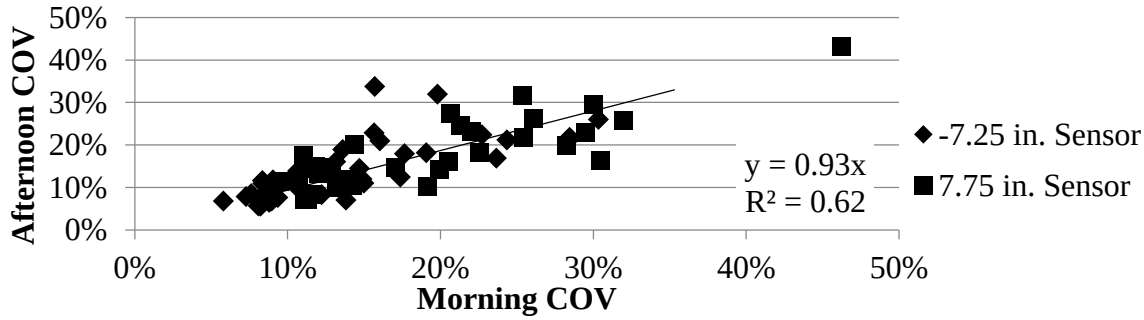

Figure 3.25 Precision Variation of RWD at Different Temperatures

3.2.2 TSD Precision Results

The TSD precision analyses were carried out based on deflection slopes as explained before. Precision of the deflection slope varied with spacing as presented in figures 3.26 through

figure 3.33. The median of the best-fit slopes for all sensors is greater than 95%, indicating that the replicate data are in general agreement. The R^2 values of the relationships between different passes are in excess of 0.9 for the first three sensors, indicating high certainty in the repeatability of the results from different passes. The farthest three sensors (including the sensor spaced at 60 inches that is not shown here) yielded median R^2 values that are less than desirable. A study by the manufacturer to assess the sources of the uncertainties of the last three sensors is warranted. The median SEE values were less than 1 mil/ft for the Mainline sections and less than 2.5 mil/ft for the Low Volume Road sections. The repeatability of the sensor located at 36 inches might be of concern given that most of the measured deflection slopes were less than 3 mil/ft

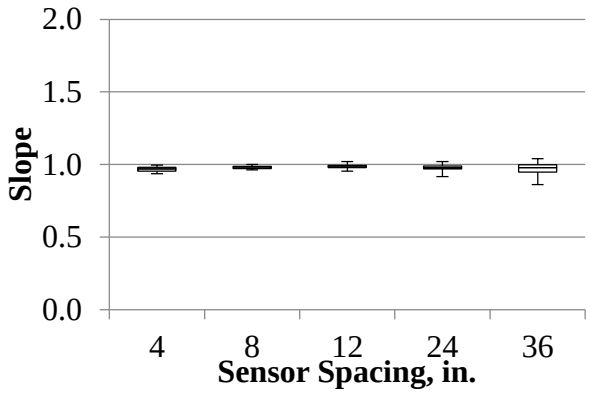

Figure 3.26 TSD Overall Precision Slope in the Low Volume Road

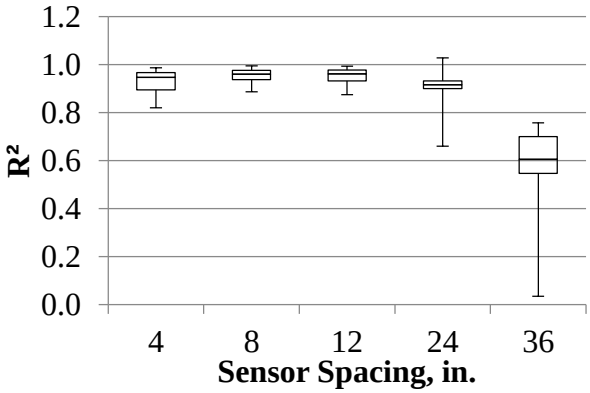

Figure 3.27 TSD Overall Precision R^2 in the Low Volume Road

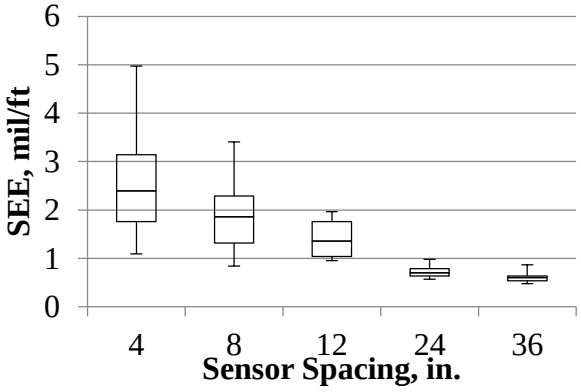

Figure 3.28 TSD Overall Precision SEE in the Low Volume Road

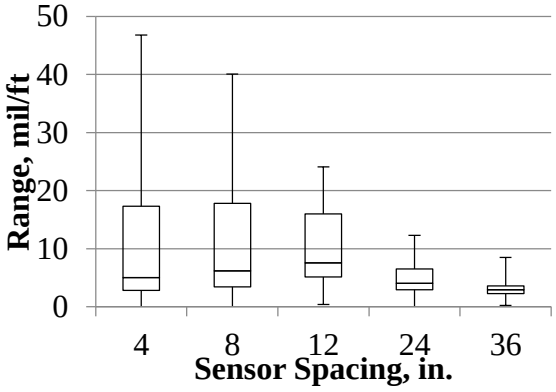

Figure 3.29 TSD Overall Precision Range in the Low Volume Road

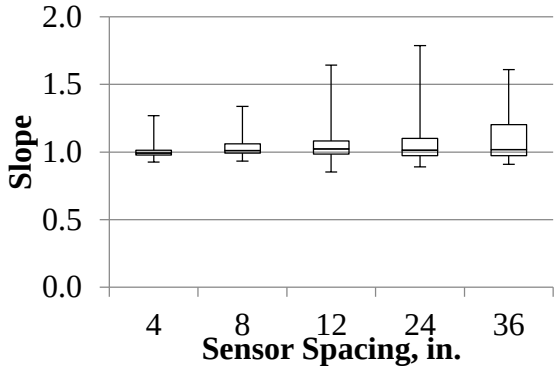

Figure 3.30 TSD Overall Precision Slope in the Mainline

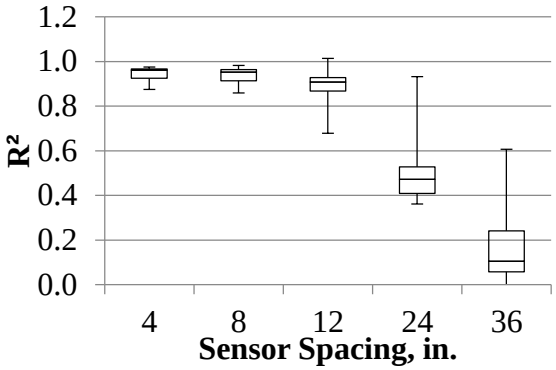

Figure 3.31 TSD Overall Precision R^2 in the Mainline

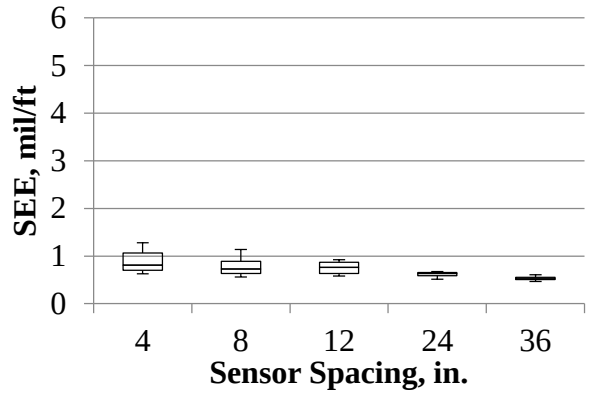

Figure 3.32 TSD Overall Precision SEE in the Mainline

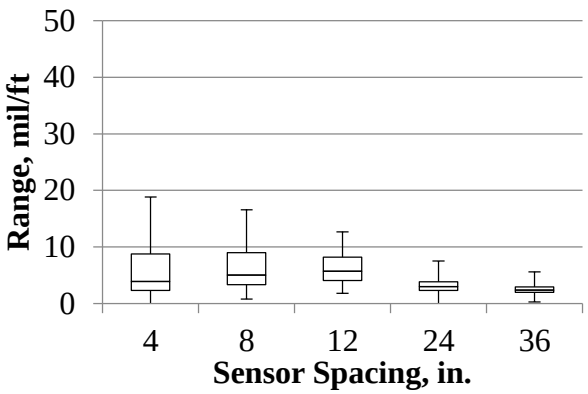

Figure 3.33 TSD Overall Precision Range in the Mainline

Figure 3.34 through 3.37 presents the overall TSD results from the Wright County 18-mile loop data averaged at a 32 ft spacing. The precision of the TSD along the 18-mile loop is similar or slightly worse in comparison to the MnROAD sections. The slopes of the best fit lines between repeat passes are greater than 0.92, but the R^2 values are less than 0.8. The SEE gradually decreases from 1.3 to 0.6 mil/ft while the median range decreases from about 8 to 4 mil/ft. Once again the precision of the farther sensors is of concern.

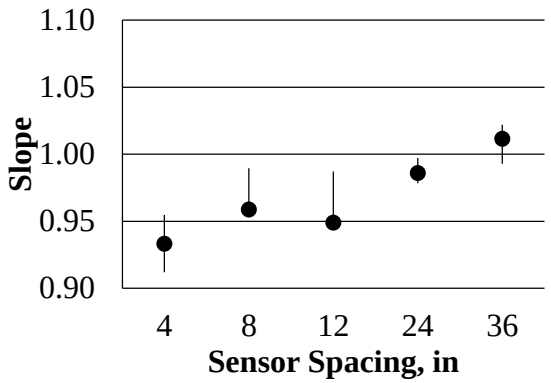

Figure 3.34 TSD Overall Precision Slope in the 18-Mile Loop

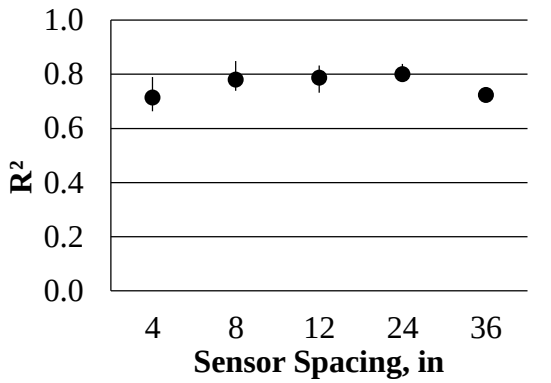

Figure 3.35 TSD Overall Precision R^2 in the 18-Mile Loop

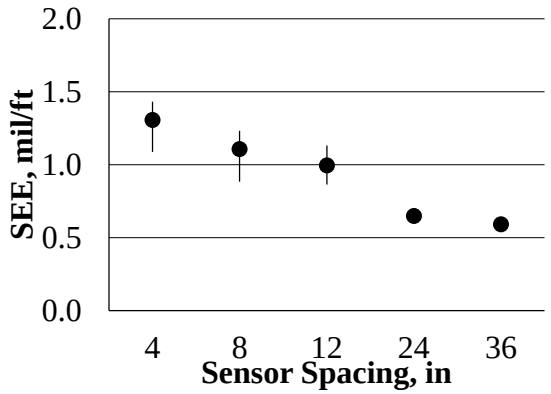

Figure 3.36 TSD Overall Precision SEE in the 18-Mile Loop

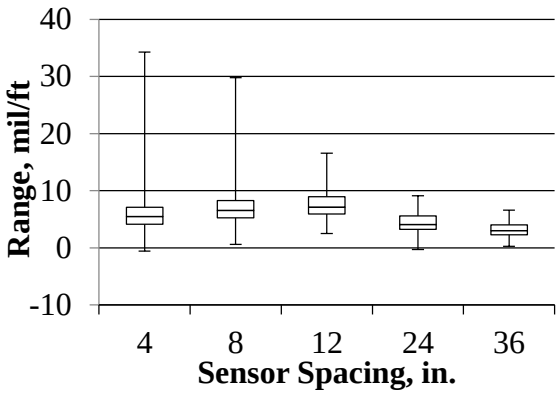

Figure 3.37 TSD Overall Precision Range in the 18-Mile Loop

Figure 3.38 and 3.39 depicts the relationships between the median COV of the deflection slope for each cell and the average FWD deflection as a surrogate for the overall stiffness of the pavement structures. The spatial COVs associated with the first four sensors tend to decrease as the FWD central deflection increases for the flexible pavements. The closest sensor exhibits larger COVs than the other sensors for the rigid pavements. From figure 3.6, the accuracy of the TSD for the flexible pavements was also impacted by the pavement stiffness. The median COVs of the

deflection slopes are also correlated to the IRI measurements in figures 3.40 and 3.41. Once again a strong relationship between these two parameters cannot be observed.

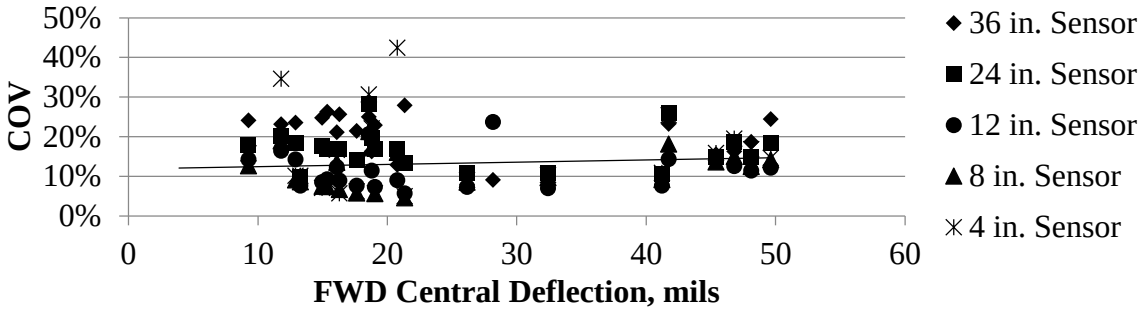

Figure 3.38 Precision Variation of TSD with Pavement Stiffness over Flexible Pavement

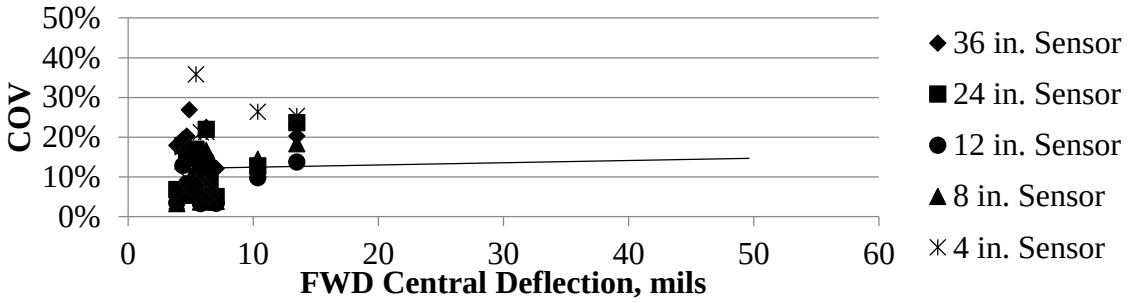

Figure 3.39 Precision Variation of TSD with Pavement Stiffness over Rigid Pavement

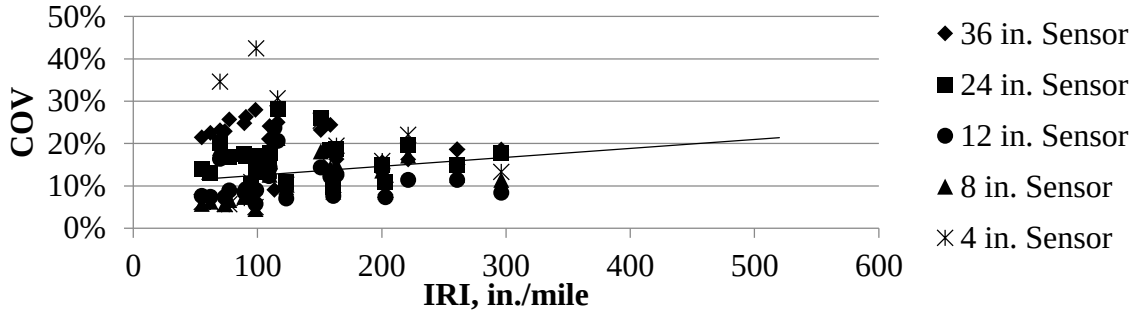

Figure 3.40 Precision Variation of TSD with IRI over Flexible Pavement

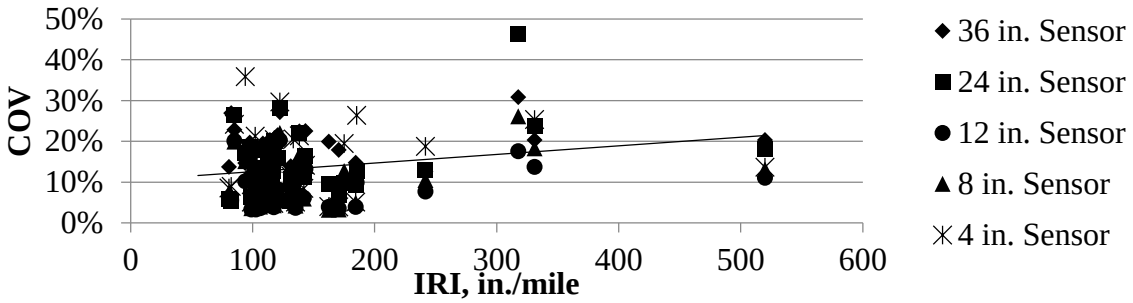

Figure 3.41 Precision Variation of TSD with IRI over Rigid Pavement

The relationships between the median COVs of the deflection slope at different vehicle speeds for the TSD are shown in figures 3.42 and 3.43. Although deflection slope was the parameter used for the TSD precision evaluation, the results appear to be affected by the vehicle speed. The COVs from tests at 30 mph along the Low Volume Road tend to be around 24% less than those measured at 45mph. The COVs from tests at 60 mph are about 38% greater than the COVs measured at 45 mph along the Mainline.

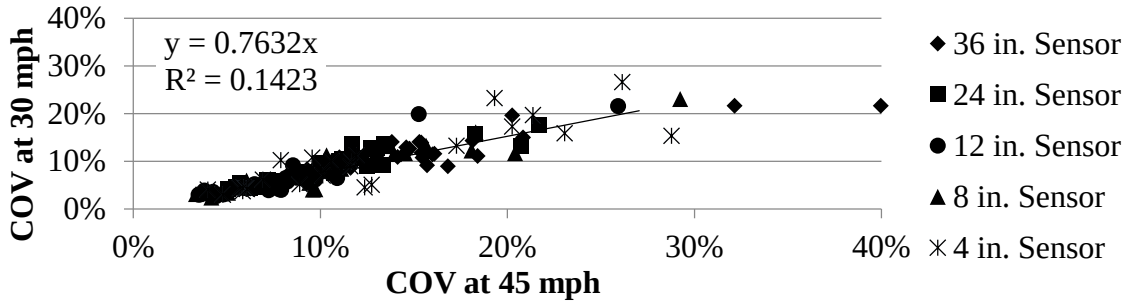

Figure 3.42 Precision Variation of TSD at Different Speeds in the Low Volume Road

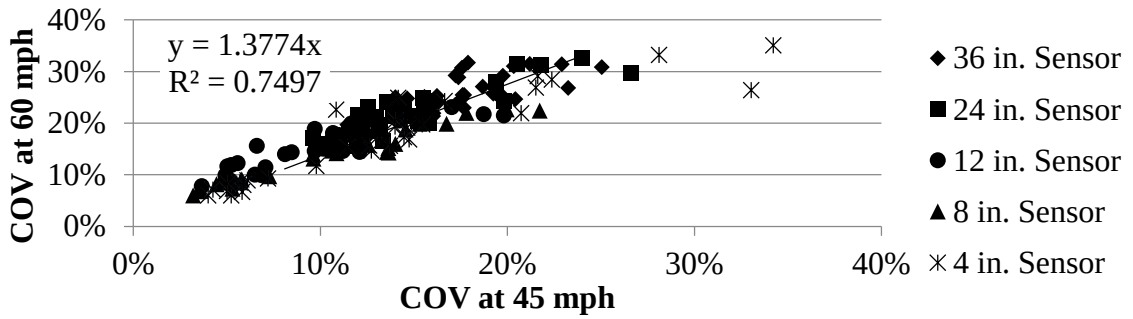

Figure 3.43 Precision Variation of TSD at Different Speeds in the Mainline

Change in pavement temperature affected the TSD differently. The precision of the TSD, presented in figure 3.44, seems to decrease with higher temperatures. Afternoon runs yielded COVs that were 32% greater than the measurements in the morning. With an R^2 value of 0.87, the precisions from the morning and afternoon tests were more correlated than from the RWD.

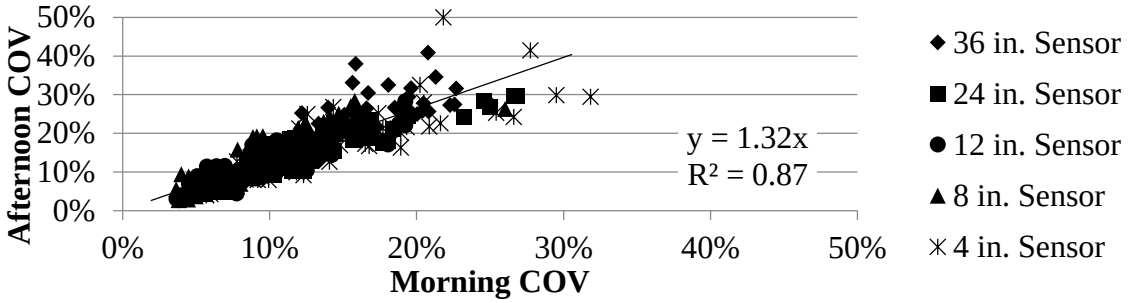

Figure 3.44 Precision Variation of TSD at Different Temperatures

Chapter 4: Summary and Conclusions

Due to the popularity of considering structural adequacy as part of the Pavement Management System Evaluation, new ways of pavement testing are needed to replace the currently widely used FWD. The objective of this thesis was to evaluate and understand the operational capabilities of three state-of-the-art pavement deflection measuring devices in terms of precision and accuracy.

This document presented the field trial locations, the instrumentation used and retrofitted to evaluate the TSDD's, the methodologies used to collect, review, reduce and analyze the data needed for quantifying the accuracy and precision of the TSDD's. Those efforts were carried out to confirm that the TSDD's meet a minimum set of specifications related to the structural evaluation of pavements at the network level.

The overall performance of the two devices was evaluated under different operating conditions including different temperatures, pavement structures and speed when feasible. The information presented in this thesis can also be used to recommend the optimum operational conditions and to identify device limitations.

The field trials took place at the MnROAD facility because it provided a multitude of test sections in one location and information readily available, including environmental and dynamic load response data. Field trial testing was also planned on an 18-mile loop located near the MnROAD facility in Wright County, MN.

In addition to the existing sensors, four geophones and one accelerometer were installed to measure deflection velocity and displacement parameters at four MnROAD cells – three flexible

cells covering a range of stiffness and one rigid pavement cell. After establishing the limitations of these sensors as used in this study, their data were used to estimate the accuracy of the TSDD's by statistically comparing the results measured with the sensors with those reported by the TSDDs at three cells for three separate repeat passes.

The precision analysis, on the other hand, included almost all cells of the MnROAD facility as well as the 18-mile Wright County Loop to account for different pavement structures and other factors such as vertical and horizontal curves. To better evaluate the precision of the TSDD's, they were tested at the MnROAD facility at different speeds and at different times of the day. Data were collected up to five times and at two different speeds. Deflection data for the replicate passes at similar speeds and times were statistically compared to estimate precision.

Based on the results presented before, the following major observations and conclusions relating to devices accuracy and precision were made:

- The RWD deflections were 11% greater than those from the embedded sensors (an SEE of 2.2 mils). It is important to recognize that in addition to the device's measurement uncertainties, there are also uncertainties associated with the embedded sensors.
- The TSD deflection velocities were 12% greater than those from the embedded sensors (with an SEE of 80mils/sec).
- With slopes between deflections from different passes averaging above 95%, measurements at all distances from the load exhibited satisfactory overall reproducibility for the two devices. The median R^2 values for the two devices was also found to be greater than 0.85 except for the farthest distances for the TSD.
- The TSD accuracy increased as the pavement stiffness decreased.

- The RWD results show some uncertainty during testing very stiff HMA section while having satisfactory results on a medium to very stiff pavement sections.
- The RWD accuracy and precision decreased as the vehicle speed increased. This was the same case for the TSD's precision, while the accuracy of the TSD increased as the speed increased.
- The TSD precision decreased when testing at high temperatures while the RWD showed lower uncertainty during the afternoon precision testing at higher temperatures

While the performance of the RWD and TSD varied under different field trials and conditions, the accuracy and precision of the RWD and TSD close to the load were considered acceptable for network-level evaluation. The precision of the measurements farther from the load for the TSD was somewhat less than desirable.

The conclusions derived from these analyses are limited by the amount of data available, the uncertainty inherent to the methodologies selected, and the assessment criteria selected by the author.

References

1. Arora, J., V. Tandon and S. Nazarian. (2006). Continuous Deflection Testing of Highways at Traffic Speeds. Technical Report No. FHWA/TX-06/0-4380-1. Texas Department of Transportation. Austin, Texas.

2. Bentsen, R. A., S. Nazarian, and J. A. Harrison. (1989). Reliability Testing of Seven Nondestructive Pavement Testing Devices. Nondestructive testing of pavements and backcalculation of moduli. ASTP-1026. Philadelphia.

3. Bryce, J., S. Katicha, G. Flintsch and B. Ferne. (2012). Analyzing Repeatability of Continuous Deflectometer Measurements. Transportation Research Board 91th Meeting. No. 12-1732. 2012. Washington, D.C.

4. Bryce, J.M., G.W. Flintsch, S.W. Katicha, and B.K. Diefenderfer. (2013). Developing a Network-Level Structural Capacity Index for Structural Evaluation of Pavements. Report No. VCTIR 13-R9. The Virginia Center for Transportation Innovation and Research.

5. Diefenderfer, B.K. (2010). Investigation of the Rolling Wheel Deflectometer as a Network-Level Pavement Structural Evaluation Tool. Report No. FHWA/VTRC 10-R5. Federal Highway Administration. Richmond, Virginia.

6. Elseifi, M., A.M. Abdel-Khalek, and K. Dasari. (2012). Implementation of Rolling Wheel Deflectometer (RWD) in PMS and Pavement Preservation. Report No. FHWA/11.492. Louisiana Department of Transportation and Development. Louisiana.

7. Fleming, P. R., M. W. Frost, and J. P. Lambert. (2015). Review of Lightweight Deflectometer for Routine in Situ Assessment of Pavement Material Stiffness. Paper No.07-1586. Transportation Research Board. Washington, D.C.

8. Flintsch, G., B. Ferne, B. Diefenderfer, S. Katicha, J. Bryce and S. Nell. (2012). Evaluation of Traffic Speed Continuous Deflection Devices. Proceedings of the 91st Meeting of the Transportation Research Board. Washington, D.C.

9. Flintsch, G., B. Ferne, B. Diefenderfer, S. Katicha, J. Bryce, S. Nell and T. Clack. (2013). Assessment of Continuous Pavement Deflection Measuring Technologies. Final Report SHRP 2 R06(F). Transportation Research Board. Washington, D.C.

10. Flintsch, G., J. Bryce and S. Katicha. (2014). Capabilities and Potential Applications of Continuous Pavement Deflection Measuring Devices. Technical Paper Geo-Congress 2014. Atlanta, Georgia.

11. Gedafa, D.S., M. Hossain, R. Miller, D.A. Steele. (2008). Network Level Pavement Structural Evaluation Using Rolling Wheel Deflectometer. No. 08-2648. 2008 87th Meeting of the Transportation Research Board. Washington, D.C.

12. Hausman, J.J and D.A. Steele. (2011). Using the Rolling Wheel Deflectometer (RWD) to Improve Pavement Management Decisions. Paper No. ICMPA170. 8th International Conference on Managing Pavement Assets. Santiago, Chile.

13. Horak E. (1987). The Use of Surface Deflection Basin Measurements in the Mechanistic Analysis of Flexible Pavements. Proceedings. Vol. 1, Sixth International Conference Structural Design of Asphalt Pavements. University of Michigan, Ann Arbor, Michigan.

14. Katicha, S.W., G.W. Flintsch, and B. Ferne. (2012). Estimation of Pavement TSD Slope Measurements Repeatability from a Single Measurement Series. Presentation in the 91st Meeting of the Transportation Research Board. Washington, D.C.

15. Kelley, J. and M. Moffat. (2012). Review of the Traffic Speed Deflectograph. Final Report AP-R395-12. AUSTROADS. Sydney NSW, Australia.

16. Rada, G.R. and S. Nazarian. (2011). The State-of-the-Technology of Moving Pavement Deflection Testing. Report No. FHWA-HIF-11-013. Federal Highway Administration. Washington, D. C.

17. Rada, G.R., S. Nazarian, B. A. Visintine, R. Siddharthan, and S. Thyagarajan. (2015) Pavement Structural Evaluation at the Network Level: Final Report. Federal Highway Administration. Washington, D.C.

Vita

Jorge Velarde came to the United States right after his high school graduation in 2009. He attended the University of Texas at El Paso to pursue a Bachelors in Civil Engineering. During his junior year he started working in the Research Center for Transportation Infrastructure Systems. Here he got involved in State and Federal research project with the chance to perform several field and laboratory test. During his undergraduate studies, he presented a research project in the Transportation Research Board Conference in Washington DC with other fellow student. Right after his bachelors' graduation, Jorge decided to pursue a Master degree in the field of Geotechnical Engineering. He was involved in a Federal Highway Administration research project in collaboration with the University of Reno, Nevada and AMEC Engineering during his graduate studies.

Permanent address: 7449 Mission Viejo
El Paso, Texas, 79912

This thesis was typed by Jorge A. Velarde Moreno